



THE HONG KONG
POLYTECHNIC UNIVERSITY

香港理工大學

Pao Yue-kong Library

包玉剛圖書館

Copyright Undertaking

This thesis is protected by copyright, with all rights reserved.

By reading and using the thesis, the reader understands and agrees to the following terms:

1. The reader will abide by the rules and legal ordinances governing copyright regarding the use of the thesis.
2. The reader will use the thesis for the purpose of research or private study only and not for distribution or further reproduction or any other purpose.
3. The reader agrees to indemnify and hold the University harmless from and against any loss, damage, cost, liability or expenses arising from copyright infringement or unauthorized usage.

If you have reasons to believe that any materials in this thesis are deemed not suitable to be distributed in this form, or a copyright owner having difficulty with the material being included in our database, please contact lbsys@polyu.edu.hk providing details. The Library will look into your claim and consider taking remedial action upon receipt of the written requests.

**Design and Analysis of Power Factor Correction
Zero-Current Switching Switched-Capacitor
Quasi-Resonant Converters**

Law Ka Kuen

**A thesis submitted in partial fulfilment
of the requirements for the Degree of**

Master of Philosophy

in

Electrical Engineering

The Hong Kong Polytechnic University

2005



**Pao Yue-kong Library
PolyU · Hong Kong**

The Hong Kong Polytechnic University

Department of Electrical Engineering

Design and Analysis of Power Factor Correction

Zero-Current Switching Switched-Capacitor

Quasi-Resonant Converters

Law Ka Kuen

A thesis submitted in partial fulfilment

of the requirements for the Degree of

Master of Philosophy

in

Electrical Engineering

Nov 2005

CERTIFICATE OF ORIGINALITY

I hereby declare that this thesis is my own work and that, to the best of my knowledge and belief, it reproduces no material previously published or written nor material which has been accepted for the award of any other degree or diploma, except where due acknowledgement has been made in the text

_____ (Signed)

Law Ka Kuen _____ (Name of student)

Abstract

In recent years, power quality is very popular in the world. Most power converters and equipment are developed to have power factor correction technology to improve their power factors. In the past research, switched-capacitor DC-DC converters were mainly used on low power applications for converting the DC voltage. They contain high switching harmonic current in the supply. In this thesis, a zero-current switched-capacitor quasi-resonant AC-DC converter with power factor correction (PFC) voltage to frequency controller is introduced. The PFC circuits provide zero-current-switching low current stress for switching components and improve high power factor over 0.9.

The voltage to frequency controller for power factor correction is shown to be stable. The control algorithm, mathematical analysis, design equations, and the circuits are discussed in details. Experimental results using aforesaid approach are demonstrated in the thesis to verify the behaviour of the design.

List of Publications

Published Journal Papers

1. K.K.Law, K.W.E.Cheng and Y.P.B.Yeung, “Design and Analysis of Switched-capacitor Based Step-up Resonant Converters”, *IEEE Transactions on Circuit and Systems*, Volume 52, Issue 5, pp. 943-948, May, 2005.
2. Y.P.B.Yeung, K.W.E.Cheng, S.L.Ho, K.K.Law and D.Sutanto, “Unified Analysis of Switched-capacitor Resonant Converters”, *IEEE Transactions on Industrial Electronics*, Volume 51, Number 4, pp. 864 – 873, Aug. 2004.

Published Conference Papers

1. Y.P..Yeung, K.W.E.Cheng and K.K.Law, “Switched-capacitor Based Step-Down Resonant Converters”, *14th Conf. of China Power Supply Society*, Sep. 2001, pp. 125-128, 2001.
2. K.W.E.Cheng, D.Sutanto, Y.L.Ho and K.K.Law, “Exploring the Power Conditioning System for Fuel Cell”, *IEEE Power Electronics Specialists Conference 2002*, Volume. 3, pp. 2197 –2202, 2001.
3. K.W.E.Cheng, K.K.Law, Y.P.B.Yeung, D.Sutanto and D.K.W.Cheng, “Development of Multiple Output Operation Based on Single Stage Switched-Capacitor Resonant Converters”, *IEEE Power Electronics Specialists Conference 2002*, Volume 3, pp. 1325 –1330, 2002.
4. K.K. Law, K.W.E Cheng, Y.P.B. Yeung and Y.Lu, "Three-Phase Power Factor Correction Using Extended-Period Quasi-Resonant Boost Converters, 10th International Power Electronics and Motion Control Conference, EPE-PEMC, 9-11 Sep 2002, Croatia.

Acknowledgements

I would like to express thanks to my supervisor, Professor Ka-Wai Eric Cheng, for his continuing guidance and encouragement throughout the course of my studies since 1999. I would also like to give thanks to everyone in my department, Department Research Committee, and Research office, especially to the Head of Department of Department of Electrical Engineering, Professor Kit Po Wong, Associate Head of Department of Electrical Engineering, Professor Siu Lau Ho, my co-supervisor, Professor Danny Sutanto, and Ms. Shirley Tsang of Research Office. I also would like to thank to everyone in my department.

A special thank goes to Mr. Raymond Choi. He has given me great technical supports and suggestions. I would give thanks to my colleagues, Dr. Benny Yeung, Mr. Y. L. Ho and my friends for their supports.

Table of Contents

Title Page	ii
Certificate of Originality	iii
Abstract	iv
List of Publications	v
Acknowledgements	vi
Table of Contents	vii
List of Figures	xi
List of Tables	xxiii
List of Key Symbols	xxiv
Chapter 1. Introduction	1
1.1. Background	1
1.1.1. Power Factor Correction Techniques	1
1.1.2. Switched-capacitor Techniques	4
1.2. Previous Researches	7
1.2.1. Zero-current and Zero-voltage Switching Converters	7
1.2.2. Power Factor Correction Converters	10
1.2.3. Switched-capacitor Converters	12
1.3. Outline of Thesis	15
Chapter 2. Zero-current Switching Quasi-resonant Switched-capacitor DC-DC Converters	17
2.1. Introduction	17

2.2. Zero-current Switching quasi-resonant Step-up Switched-capacitor DC-DC Converters	18
2.2.1. Operation Principle	19
2.2.2. Mathematical Analysis	21
2.2.3. Simulation Results	23
2.2.4. Experimental Results	25
2.3. Discussion	30
2.4. Summary	32
Chapter 3. Principles of Power Factor Correction Techniques in Zero-current Switching Quasi-resonant Switched-capacitor Conversion	33
3.1. Introduction	33
3.2. Concept of Power Factor Correction Techniques in Zero-current Switching Quasi-resonant Switched-capacitor Converters	33
3.3. Principle of Power Factor Correction Techniques in Zero-current Switching Quasi-resonant Switched-capacitor Converters	35
3.4. Family of Quasi-Resonant Switched Capacitor PFC circuits	41
3.5. DC/DC Converter Techniques for Shaping the Converters Input Current	42
3.6. Summary	45
Chapter 4. Mathematical Analysis of the Power Factor Correction Zero-current Switching Switched-capacitor AC-DC Converters	46

4.1.	Introduction	46
4.2.	Initial Analysis On Single Stage Step-up PFC Circuit	47
4.2.1.	State Equations of the Step-up Circuit	47
4.2.2.	Continuity Analysis and Energy Equation	51
4.3.	Analysis On Triple Step-up PFC Circuit	53
4.3.1.	State Equations of the Step-up Circuit	53
4.3.2.	Continuity Analysis and Energy Equation	56
4.4.	Generalised Analysis On Step-up PFC Circuit	57
4.5.	Design Methods	60
4.5.1.	Conditions of Zero-current Switching	60
4.5.2.	Selection of Resonant Components	60
4.5.3.	Rating of Component	61
4.6.	Discussion	62
4.7.	Summary	63
 Chapter 5. Control of Power Factor Correction Zero-current		 64
Switching Switched-capacitor AC-DC Converters		
5.1.	Introduction	64
5.2.	Controller Design	64
5.3.	Simulation Analysis	65
5.4.	Experimental Results	73
5.4.1.	Specification	73
5.4.2.	Operation Under DC condition	74
5.4.3.	Initial of Examination of VCO	76

5.4.4.	Examination of the AC-DC converters under various operation	76
5.5.	Summary	82
Chapter 6.	Conclusions and Recommendations	83
6.1.	Conclusions	83
6.2.	Recommendations for Further Researches	85
Appendix A	Family of zero-current switching quasi-resonant step-down switched-capacitor converters	87
References		101

List of Figures

Fig. 1.1	Passive power factor correction circuit	2
Fig. 1.2	Active power factor correction circuit	3
Fig. 1.3	Voltage inverting and the voltage step-up circuit	5
Fig. 1.4	Circuit diagrams of switched-capacitor step-up converters	12
Fig. 2.1	Circuit diagrams of zero-current switching quasi-resonant step-up converters	18
Fig. 2.2	States of operation of triple-mode switched-capacitor resonant converter	19
Fig. 2.3	Simulation waveforms of triple mode switched-capacitor resonant converter	24
Fig. 2.4	Measured waveforms of triple mode switched-capacitor resonant converter	26-28
Fig. 2.5	Measured efficiency and output power of the triple mode switched-capacitor resonant converter	29
Fig. 3.1	Principle control block diagram	36
Fig. 3.2	Variable output frequency waveform of the PFC controller	36
Fig. 3.3	Step-up PFC circuit	38
Fig. 3.4	Step-down PFC circuit	39
Fig. 3.5	Inverting mode PFC circuit	40
Fig. 3.6	PFC circuit with shaping DC/DC converter	42
Fig. 3.7	Step-up PFC circuit with shaping DC/DC converter	43

Fig. 4.1	Schematic of the power factor correction circuit using double mode step-up version.	47
Fig. 4.2	Equivalent circuit during 4 stages of operation	48
Fig. 4.3	Circuit of the step-up triple circuit with shaping DC/DC converter	53
Fig. 4.4	n-mode circuit for the AC-DC power conversion with shaping DC/DC converter	57
Fig. 5.1	Circuit diagram of power factor correction controller for zero-current switching switched-capacitor quasi-resonant AC-DC converter	65
Fig. 5.2	Relationship between the main input voltage and PFC controller gate signal frequency	65
Fig. 5.3	PFC controller gate signal frequency at main input voltage equal to 0V	66
Fig. 5.4	PFC controller gate signal frequency at main input voltage equal to 20V	67
Fig. 5.5	PFC controller gate signal frequency at main input voltage equal to 40V	67
Fig. 5.6	Resonant current at main input voltage equal to 0V	68
Fig. 5.7	Resonant current at main input voltage equal to 30V	68
Fig. 5.8	Resonant current at main input voltage equal to 40V	69
Fig. 5.9	Relationship of resonant current, main input voltage and switching frequency of PFC controller	70

Fig. 5.10	Outline of the simulation result for Triple-mode PFC ZCS quasi-resonant switched-capacitor AC-DC converter	70-72
Fig. 5.11	Circuit block diagram of power factor correction zero-current switching switched-capacitor triple-mode quasi-resonant AC-DC converters with shaping DC/DC converter	73
Fig. 5.12	Measured result of resonant inductor current at difference switching frequency	75
Fig. 5.13	Measured relationships between the main input voltage and PFC controller gate signal frequency	76
Fig. 5.14	Measured input voltage and current of triple-mode PFC zero-current switching quasi-resonant switched-capacitor AC-DC converter	77
Fig. 5.15	Measured efficiency and output power of triple-mode PFC zero-current switching quasi-resonant switched-capacitor AC-DC converter	78
Fig. 5.16	Measured voltage conversion Ratio and output power of triple-mode PFC zero-current switching quasi-resonant switched-capacitor AC-DC converter	79
Fig. 5.17	Measured efficiency and output power of triple-mode PFC zero-current switching quasi-resonant switched-capacitor AC-DC converter	79
Fig. 5.18	Measured power factor and output power of triple-mode PFC zero-current switching quasi-resonant switched-capacitor AC-DC converter	80

Fig. 5.19	<i>Measured THD and output power of triple-mode PFC zero-current switching quasi-resonant switched-capacitor AC-DC converter</i>	80
Fig. A1	<i>Circuit diagrams of zero-current switching quasi-resonant step-down converters</i>	87
Fig. A2	<i>Circuit diagrams of zero-current switching quasi-resonant inverting mode converters</i>	88
Fig. A3	<i>Switched-capacitor cell for step-up mode</i>	89
Fig. A4	<i>States of operation of inverting -1/2-mode switched-capacitor resonant step-down converter</i>	90
Fig. A5	Measured waveforms of the inverting 1/2-mode switched-capacitor resonant step-down converter	96-97
Fig. A6	Measured efficiency and output power of the inverting 1/2-mode switched-capacitor resonant step-down converter	100
Fig. A7	Measured voltage conversion Ratio and output power of the inverting 1/2-mode switched-capacitor resonant step-down converter	100

List of Tables

Table 2.1	Variable of the simulation waveform	24
Table 2.2	Specification of Prototype of Triple-mode Converters	25
Table 2.3	Measured efficiency, input and output value of the triple mode switched-capacitor resonant converter	29
Table 5.1	Design specification of Controller	64
Table 5.2	Measured result of triple-mode PFC zero-current switching quasi-resonant switched-capacitor AC-DC converter at difference switching frequency	74
Table A1	Specification of Prototype of Inverting 1/2-mode Converters	95

List of Key Symbols

$V_{in} = V_s$	Input Voltage	ω	AC Source Frequency
L_f	Filtering Inductor	V_{g1}	Gate Signal of S_1
C_f	Filtering Capacitor	V_{g2}	Gate Signal of S_2
C_o	Output Capacitor	V_{ds1}	Vds of FET S_1
I_o	Output Current	V_{ds2}	Vds of FET S_2
I_{in}	Input Current	V_{c1}	Voltage of Capacitor C_1
R_L	Load Resistor	V_{c2}	Voltage of Capacitor C_2
C_1, C_2	Resonant Capacitor	G_1	Gain of Switching Capacitor Converter
S_1, S_2	Switching Device (FET)	G_2	Gain of DC/DC Converter
L_r	Resonant Inductor	V_{stack}	Output of DC/DC Converter
C_{1a}, C_{1b}	Resonant Capacitor	P_1	Power of Switching Capacitor Converter
C_{2a}, C_{2b}	Storage Capacitor	P_2	Power of DC/DC Converter
D_{1a}, D_{1b}	Diode	P_o	Output Power
D_{2a}, D_{2b}	Diode	I_A	Amplitude of Resonant Current at Period A
V_o	Output Capacitor	I_B	Amplitude of Resonant Current at Period B
i_{Lr}	Resonant Inductor Current	d_1	Duty Ratio of S_1
V_{c1a}	Voltage of Capacitor C_{1a}	d_2	Duty Ratio of S_2
V_{c1b}	Voltage of Capacitor C_{1b}	k	VCO Variable and function of t
T_s	Period of Source Voltage	T_o	Period of Resonant Tank
ω_0	Frequency	L	Inductor
Z_0	Impedance	C	Capacitor

Chapter 1 Introduction

1.1. Background

This thesis studies power factor correction (PFC) zero-current switching switched-capacitor quasi-resonant AC-DC converters with voltage-controlled-frequency technique. This session introduces briefly the backgrounds of these technologies.

1.1.1 Power Factor Correction Techniques

Most single-phase AC-DC switched-mode power converters operate effectively with small size and light weight. Due to these advantages, they were widely used in commercial, industrial, aerospace, residential and military applications recently [1.1]. It is known that an AC-DC power converter without PFC connected to an AC main power supply introduces harmonic current. It is mainly because the proliferation of the AC-DC power converter draws pulsating input current. The harmonic current injecting to the AC main power supply causes several problems such as

- Reducing the capability of the power line to providing energy,
- Leading to voltage distortion, and
- Inducing heat and conduction losses on the switching components [1.2-1.4].

PFC techniques can be used in AC-DC power converters to improve the power quality. In general, PFC techniques can be classified into two categories. The first technique is passive PFC technique. This technique consists of inductor-capacitor (LC) filter which is connected in either AC main power supply or DC rectifier output of the AC-DC power converters to reduce the harmonic input current shown in Fig. 1.1. This technique is very simple of high efficiency, high reliability and low cost. However, the LC-filter is bulky and heavy. Besides, it cannot achieve very high power factor.

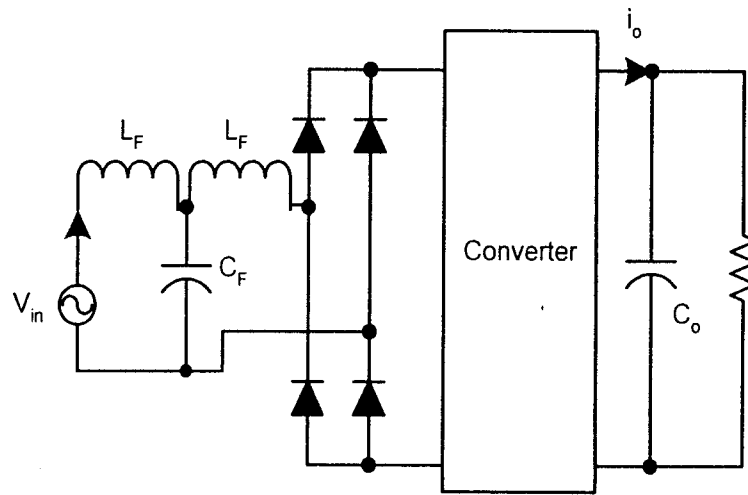


Fig. 1.1 Passive power factor correction circuit

Another technique is active PFC technique. This technique can obtain nearly unity power factor by shaping input current of power converters to sinusoidal and in-phase with the input voltage [1.5]. Advantages include configuration in lightweight and high power factor. By means of the current shaping method, the current harmonics at the input can be improved and hence the total harmonic distortion can be also reduced.

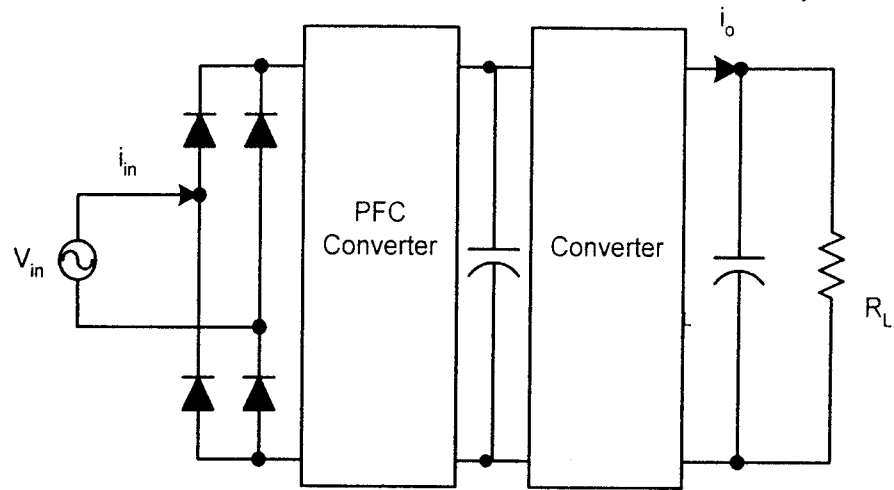


Fig. 1.2 Active power factor correction circuit

The active PFC techniques have three techniques and two classes of control strategies. The active PFC techniques include hard-switching pulse-width-modulation (PWM) PFC technique, resonant technique and soft-switching PFC technique [1.1]. Control strategies include current mode control and voltage mode control. Current mode control refers to charge control, non-linear carriers' control, hysteresis control [1.6], peak current control, and average current control [1.2]. Voltage mode control refers to capacitor voltage control and inductor voltage control.

1.1.2 Switched-capacitor Techniques

Switched-capacitor voltage converters accomplish energy transfer and voltage conversion using capacitors [1.7]. Most of the two common switched-capacitor voltage converters are voltage inverting circuit and the voltage doubling circuit as shown in Fig. 1.3. Switched-capacitor converters are widely used in switched mode power supplies (SMPS) for power conversions, conditionings and are suitable for custom IC implementation. Regarding the voltage inverting circuit, the switched capacitor, C_1 is charged to the input voltage during the first half switching cycle. During the second half switching cycle, its voltage is inverted and applied to the output capacitor C_2 and the load. The output voltage is negative to the input voltage. The average input current is approximately equal to the output current. The switching frequency has a large impact the size of the resonant capacitors [1.8]. Higher switching frequency allows using smaller switched capacitors. The duty cycle is defined as the ratio of charging time for C_1 to the entire switching cycle. It is usually near and less than 50% because that generally yields the optimal charge transfer efficiency.

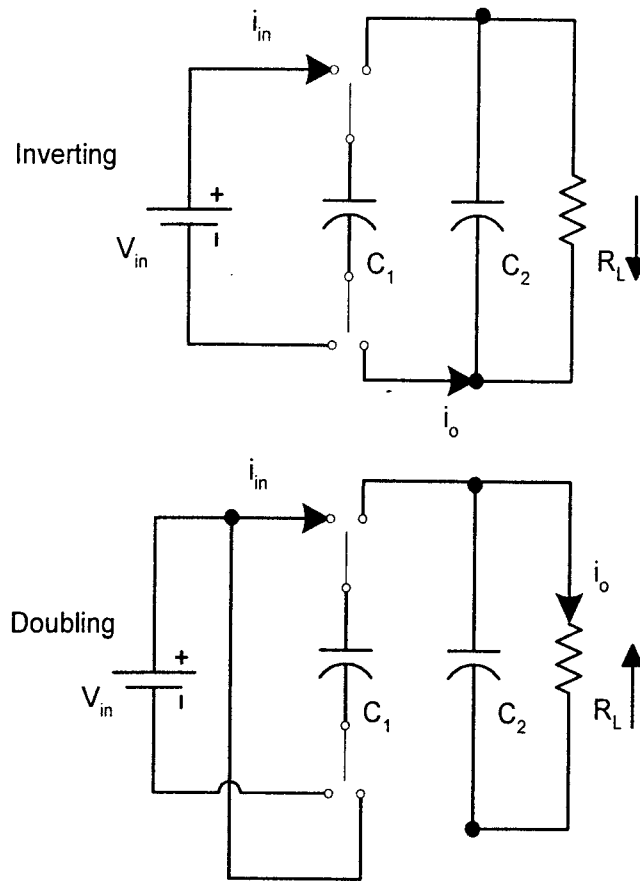


Fig. 1.3 Voltage inverting and the voltage step-up circuit

In steady-state condition, only the charge resonant capacitor has to supply a small amount of charge to the output capacitor on each switching cycle. The amount of charge transfer depends upon the load current and the switching frequency. When the input voltage charges the switched capacitor, the output capacitor C_2 must supply the load current. The load current flowing out of C_2 causes a drop of the output voltage that corresponds to a component of output voltage ripple. Higher switching frequency allows using smaller capacitors for the same amount of droop. However, the switching speeds, switching losses and switching frequencies are generally limited to a few hundred kHz in practice [1.10].

The voltage doubling circuit works similarly to the voltage inverting circuit; however, the switched capacitor is configured in series with the input voltage during its discharge cycle, thereby accomplishing the voltage doubling function. The average input current of this circuit is approximately twice of its average output current.

There are certain advantages and disadvantages for the conventional switched-capacitor voltage converters. In addition, these circuits are simple. Each circuit usually needs two or three capacitors only. Obviously, the current output is limited by the size of the capacitors and the current carrying capacity of the switches. However, they cannot maintain high efficiency for a wide range of ratios of input to output voltages, unlike their switching regulator counterparts [1.9]. This is because the input to output current ratio is scaled according to the basic voltage conversions. More additional capacitors are required for high conversion ratio as the capacitors have equivalent series resistance (ESR) [1.11]. Practically, all capacitors have equivalent series resistance (ESR) and equivalent series inductance (ESL). These parasitic may affect the ability of the capacitor to store charge under high switching frequency. Also, ESR affects the overall efficiency of the switched-capacitor voltage converter. Various sources of power loss in switched-capacitor voltage inverting and doubling circuits are inherent by the ESR of the switched-capacitor, resistances associated with each switch, as well as the ESRs of the filtering capacitors.

1.2. Previous Researches

This section is going to review the previous research of basic operation of PFC converters, switched-capacitor converters and zero-current switching converters.

1.2.1 Zero-current and Zero-voltage Switching Converters

There are many soft-switching techniques available in literatures that mention the improvement of the switching behaviour of dc-to-dc resonant converters. The intensive research in soft-switching is under way to further improve efficiency with increased switching frequency of power electronic circuits. Using the resonant PWM switches to achieve zero-switching condition are very popular nowadays. For simplicity, using the zero-switching techniques refer to DC-DC converters, quasi-resonant converters while other topologies apply resonance to reduce switching losses. Two major techniques are generally employed to achieve low switching losses, such as zero-current switching (ZCS) technique and zero-voltage switching (ZVS) technique [1.13]. This session will focus on well-known types of PWM resonant switches and their steady state analyses.

For ZCS techniques, the power switch turn-OFF at zero-current but at turn-ON, the converter still suffers from the capacitor turn-ON loss caused by internal conduction of the output capacitor of the power switch.

In general, most regulator converter switches need to turn ON or turn OFF the full load current at high voltage, resulting in what is known as hard-switching. The typical switching loci for a hard-switching converter are rectangular and this implies higher loss.

For many years, high efficiency power processing circuits has been achieved by operating power semiconductor devices in the switching mode, whereby switching devices are operated in either the ON or OFF states as in the PWM method. In PWM converters, switching of semiconductor devices normally occurs at high current levels [1.15]. Therefore, when switching at high frequencies these converters are associated with high power dissipation in their switching devices. Furthermore, the PWM converters suffer from EMI caused by high frequency harmonic components associated with their quasi-square switching current and/or voltage waveforms with today's power semiconductor and circuit technology, PWM converters can operate up to Mega Hz. Unfortunately, although the technological advancement of PWM switch mode converters has resulted in faster switching devices, their operating frequency is limited by the reasons mentioned above.

For both ZCS and ZVS techniques, the switching losses in the semiconductor devices are avoided due to the fact that current through or voltage across the switching device at switching instant is equal to or near zero. The reduction in the switching loss allows the designer to attain a higher operating frequency without sacrificing converter efficiency. By means of this approach, the resonant converters are able to achieving performance that cannot be achieved by the PWM

converter. This is the design rule of thumb of small size and weight converters. Currently, resonant power converters operating in the range of a few megahertz are available. Another advantage of resonant converters over PWM converters is the decrease of harmonic content in the converter voltage and current waveforms [1.16]. Therefore, when the resonant and PWM converters are operated at the same power level and frequency, it is expected that the resonant converter will have lower harmonic emission.

The major advantage of ZCS and ZVS quasi-resonant converters is that the power switch is turned ON and OFF at Zero-Voltage and Zero-Current respectively. In ZCS topologies, the rectifying diode may also have ZVS or ZCS operation while in ZVS topologies, the rectifying diode may also have ZCS or ZVS operation.

The second advantage is that both ZVS and ZCS utilize transformer leakage inductance and diode junction capacitors and output parasitic capacitor of the power switch [1.17]. The major disadvantage of ZVS and ZCS techniques is that they require variable-frequency control to regulate the output. This is undesirable since it complicates the control circuit and generates unwanted EMI harmonics, especially under wide load variations. In ZCS, the power switch turns OFF at zero-current but at turn-ON, the converter still suffers from the capacitor turn-ON loss caused by the output capacitor of the power switch. However, it is suitable for handling high current operation.

1.2.2 Power Factor Correction Converters

Recently, PFC techniques and control strategies are very common for application. Power factor correction can be accomplished by any one of the numerous power conversion techniques. Nowadays, it is very common that using boost topology operating in continuous conduction mode (CCM) for high power applications and discontinuous conduction mode (DCM) for lower output power applications. The drawbacks of this approach are that the output voltage of the boost converter must be greater than the input peak voltage and the input and output of the circuit are non-isolated. In flyback topology, the output voltage can be greater than or less than the input peak voltage depending on the turn ratio of the transformer. A simple buck regulator has also been proposed for PFC and it provides lower output voltage than the input voltage for non-isolated application with sound results. However, it still suffers from discontinuous current at the input because the main switch is in series with the input. In continuous inductor current boost topology, fixed conversion frequency and current mode control are usually used.

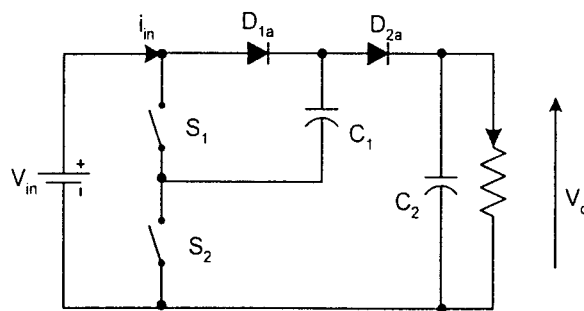
There are two common control techniques for PFC. They are peak current mode control and average current mode control. However, conventional peak current mode control is difficult to be implemented because it is necessary to add slope compensation for stability over the wide range of duty cycles. Average current mode control can eliminate the need of slope compensation, and can additionally optimize the dynamic response of the pre-regulator. Another type of continuous current technique is hysteretic current control. The inductor current

is switched to follow a peak and valley current level which tracks the sinusoidal supply voltage shape and associated current. The hysteresis can be a fixed amount or proportional to the instantaneous average current. Variable frequency operation of the switch is required to accommodate the hysteresis, which may require synchronization and also some careful filter design consideration

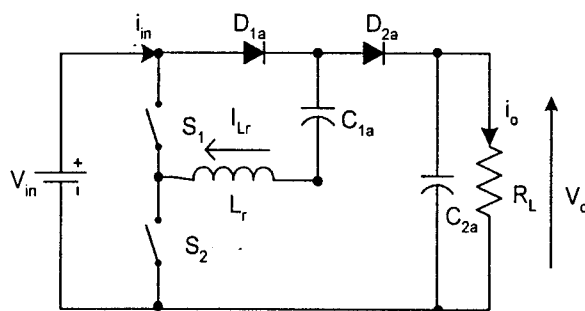
PWM for PFC converters have advantages such as simple configuration, low voltage and current stress, ease analysis and control. This approach requires the switching component operating at PWM mode with high frequency so that the size of the AC-DC power converters is small. Therefore, it is extensively used in PFC circuit. Combining PWM PFC techniques in the resonant converter, PFC with soft-switching or zero-current switching can be achieved.

1.2.3 Switched-capacitor Converters

Conventional switched-capacitor converters are very commonly used for low power supply systems. The conventional switched-capacitor converters were shown in Fig. 1.3. In principle, these converters are with features including using capacitors as the energy storage components, and controlling the path of charging and discharging of the capacitors by the switching devices to achieve the different voltage conversion ratios. The main advantages of this type of converters are without magnetic components, low cost, compact, low profile and possibility to be fabricated in integrated chips [1.9].



(a) Conventional Double Mode



(b) Resonant Double Mode

Fig. 1.4 Circuit diagrams of switched-capacitor step-up converters

The resonant double mode switched-capacitor converter can obtain the high efficiency compare with the conventional type of switched-capacitor converter and this technique has to control the charged and discharged of the resonant capacitors in fixed periods. Fig.1.4(b) shows the resonant circuit and its operation is very similar to that of the conventional double mode on Fig. 1.4 (a). The switch S_1 and S_2 are turned on and off alternatively. The operation is explained here by using the topology of Fig. 1.4. When S_2 is turned on, D_{1a} are forward biased. C_{1a} is in series resonance with L_r through D_{1a} and C_{1a} is charged by V_{in} .

When S_1 is turned on in the second-half switching cycle, D_{1a} is reverse biased and D_{2a} is forward biased. Hence, C_{1a} is connected in series with L_r and source V_{in} to charge the output capacitor C_{2a} in double of V_{in} . Both S_1 and S_2 are turned on and off under zero-current switching to reduce the switching stress of the switching device of the converters.

Fig. 1.4 shows the circuits of the conventional and resonant double mode step-up converters. The main shortcomings of the conventional switched-capacitor converters are that the switching devices of the converters operate under very high current stress [1.7]. It is because the capacitors are connected directly to the charging source and output filtering capacitor during charging and discharging respectively. The number of the switching devices of converters is large if the switched-capacitor converter is designed for high voltage conversion ratio [1.7]. Hence, the converters efficiency is low and control of the device is more extensive. Moreover, most conventional switched-capacitor

converters circuits have an inherent drawback such that their efficiencies much decrease when their output currents increase. Some operations of the conventional switched-capacitor converter are based on the transistor working in non-saturation mode in order to regulate the voltage and therefore the loss of these converters is high. These converters are therefore usually used only for low power and operating at lower efficiency. The efficiency also deteriorates seriously as the switching frequency increases.

The conventional switched-capacitors converter is usually designed in an uncontrolled manner of leakage inductance in the circuit, as a result, high current stress and spikes problems can be observed and it causes high electromagnetic interference (EMI) of the voltage source when the switched-capacitors are being charged and discharged. These kinds of converters have no magnetic components. They use capacitors for storing energy so that the size of the converter is small. Also, it can be fabricated in integrated circuit chips or very low profile system.

1.3. Outline of Thesis

The background of the design techniques and previous converters operation topology has been introduced for developing the new proposed power factor correction of zero-current switching quasi-resonant switched-capacitor AC-DC converters with voltage-controlled-frequency control technique. The main results and contribution of this thesis are outlined as follows: -

- (i) Propose the step-up zero-current switching quasi-resonant switched-capacitor DC-DC converters had been analysed and introduced in Chapter 2. The converters are operated under zero-current condition and quasi-resonance. In Chapter 2, the operation principles, the mathematical analysis and the simulation results will be explained as well as the experimental tests of the prototype circuit will be provided.
- (ii) In Chapter 3, a new concept and the operation principles PFC techniques in zero-current switching quasi-resonant switched-capacitor AC-DC converters will be introduced.
- (iii) In Chapter 4, the design methods, switching devices operation conditions, selection of components rating and power losses analysis will be explained for PFC zero-current switching quasi-resonant switched-capacitor AC-DC converters. The mathematical analysis will be introduced for design and further discussion.

- (iv) In Chapter 5, a new controller for improving the power factor in zero-current switching quasi-resonant switched-capacitor AC-DC converters will be explained. A high power operation of the proposed PFC zero-current switching quasi-resonant switched-capacitor AC-DC converters will be experimented and discussed. Mathematical analysis and computer simulation will be carried out for discussion.
- (v) Conclusions and recommendations will be provided in Chapter 6. The further study and research for the PFC quasi-resonant switched-capacitor AC-DC converters with voltage-controlled-frequency technique are recommended.

Chapter 2 Zero-current Switching Quasi-resonant

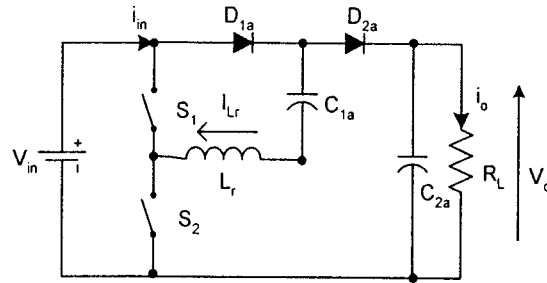
Switched-capacitor DC-DC Converters

2.1. Introduction

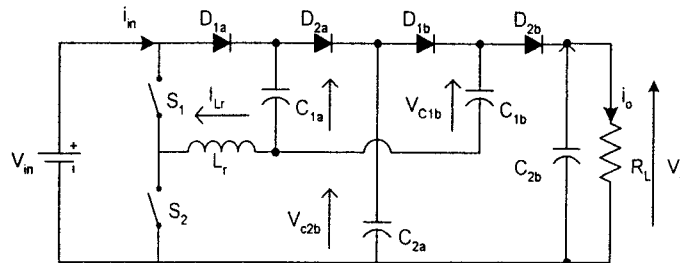
In recent years, switched-capacitor converters are widely used in switched mode power supplies (SMPS) for power conversions and conditionings in low power applications. It is because the conventional SMPS are consisting of large magnetic components, such as inductors or transformers for energy storage and conversions. Hence, the weight and the size of the converter structure are usually reduced as well as the component profile.

In this chapter, a step-up zero-current switching switched-capacitor resonant converter is presented. These converters have both the advantages of conventional SMPSs and switched-capacitor converters. The circuits consist of only two switching devices, some diodes and a number of switching-capacitor cells, which can improve the aforesaid problem. All switching devices inside circuit are switch-ON and switch-OFF under zero-current switching condition by the resonance of the switched-capacitors and a very small resonant inductor. The resonant currents of the proposed converters are used as assisting zero-current switching in quasi-resonant manner [2.1]. The capacitor charging and discharging currents are half sinusoidal waves. Hence, the current spike problem can be solved [2.2].

2.2 Zero-current Switching quasi-resonant Step-up Switched-capacitor DC-DC Converters



(a) Double-mode



(b) Triple-mode

Fig. 2.1 Circuit diagrams of zero-current switching quasi-resonant step-up converters

The proposed circuit diagrams of step-up mode zero-current switching quasi-resonant switched-capacitor DC-DC converters as shown in Fig 2.1. The converter provides different output voltages by adding the some diodes and capacitor [2.3]. Diagrams of different operation principles for various voltage conversion mode circuits of the zero-current switching quasi-resonant switched-capacitor DC-DC converters are shown in Fig. 2.2 and four operation states of the proposed triple-mode step-down zero-current switching quasi-resonant switched-capacitor converter are analysed.

2.2.1. Operation Principle

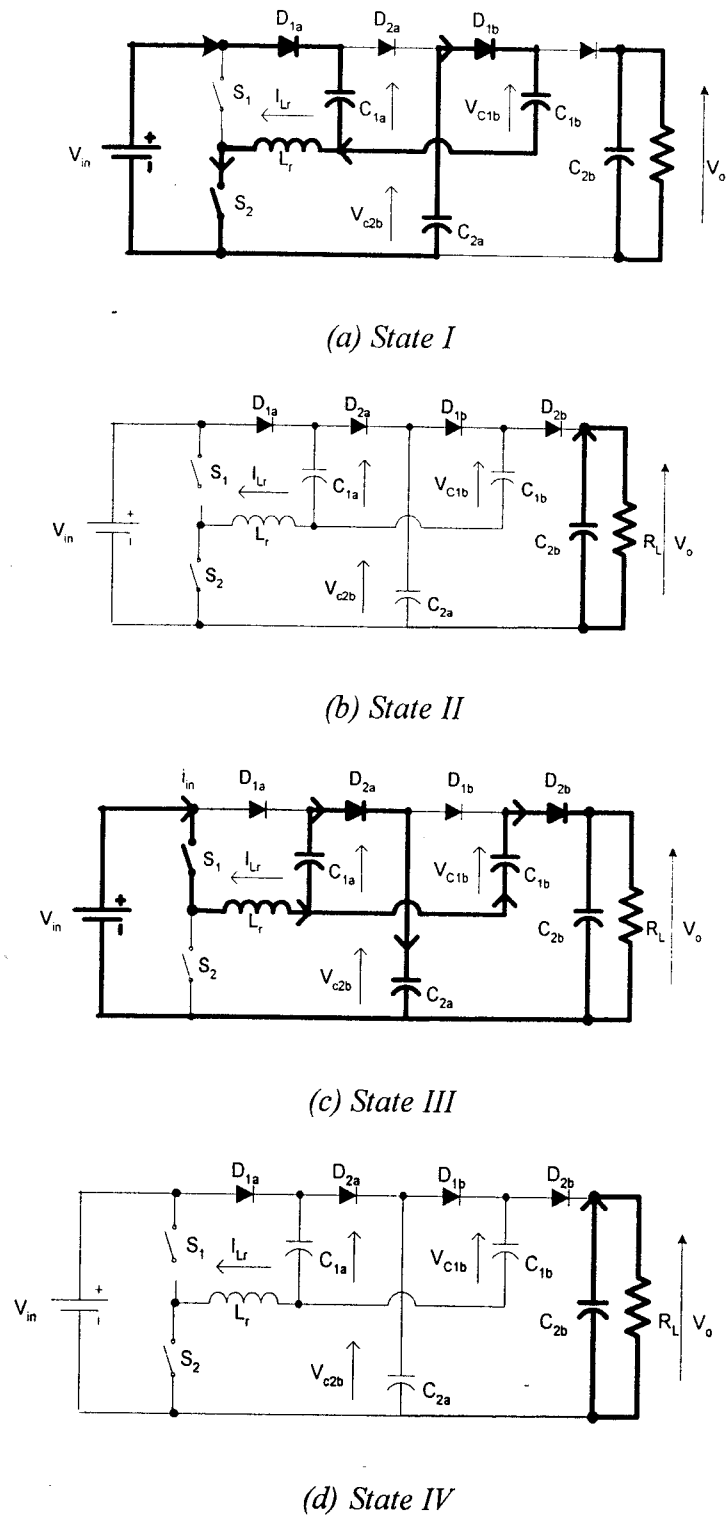


Fig. 2.2 States of operation of triple-mode switched-capacitor resonant converter

Fig. 2.2 shows equivalent circuits of each state of operation of the triple-mode switched-capacitor resonant step-up converter.

(i) *State I* [$t_0 - t_1$]

S_2 is switched on and S_1 is switched off in this state. C_{1a} and L_r resonate together with V_{in} while C_{1b} and L_r resonate together with C_{2a} . They all start resonating at t_0 from the current equal to zero in sinusoidal manner. Since the current increases gradually at t_0 , S_2 is switched on under zero-current switching condition. They stop resonating when the current reaches zero again at t_1 by the reverse biased D_{1a} and D_{1b} . Let $L_r = L$ and $C_{1a} = C_{1b} = C$. C_{2a} and C_{2b} are assumed to be large enough to keep the voltage to be constant, and the circuit is assumed to be lossless.

(ii) *State II* [$t_1 - t_2$]

Both S_2 and S_1 are still switched off in this state. The resonance stops at t_1 . The inductor current is equal to zero. The voltages of C_{1a} , C_{1b} and C_{2a} are unchanged. C_{2b} discharges to the load. At t_2 , S_1 is switched on and S_2 is switched off. Hence, S_2 is switched off under zero-current condition.

(iii) *State III* [$t_2 - t_3$]

S_1 is switched on and S_2 is switched off in this state. L_r and C_{1a} resonate in series together and connected with source V_{in} to C_{2a} while L_r resonates with C_{1b} and connected together to C_{2b} and the load. Similar to State I, the resonant

currents are in sinusoidal manner. They increase from zero at t_2 gradually so that zero-current turn-on of S_1 is achieved. The current reaches zero at t_3 . The resonance stops by the reverse biased diodes D_{2b} and D_{2a} .

(iv) *State IV* [$t_3 - t_4$]

In this state, both S_1 and S_2 are still switched off. Similar to State III, the resonance stops at t_3 . The instantaneous inductor current is equal to zero. The voltage of C_{1a} and C_{1b} is unchanged. C_{2b} discharge to the load again. At t_4 , S_2 is switched on and S_1 is switched off. Hence, S_1 is switched off in zero-current condition.

2.2.2 Mathematical Analysis

(i) The equations of State I [$t_0 - t_1$] can be derived by classical circuit equation: -

Voltage source $V_{in} = V_s$

$$v_{C1a} = V_s - \frac{3}{4} I_o T_s \omega_0 Z_0 \cos \omega_0 (t - t_0) \quad (2.1)$$

$$i_{Lr} = \frac{3}{4} I_o T_s \omega_0 \sin \omega_0 (t - t_0) \quad (2.2)$$

$$v_{C1b} = 2V_s - \frac{3I_o T_s \omega_0 Z_0}{4} \cos \omega_0 (t - t_0) \quad (2.3)$$

Where,

$$\omega_0 = \frac{1}{\sqrt{2LC}} \quad (2.4)$$

$$Z_0 = \sqrt{\frac{L}{2C}} \quad (2.5)$$

(ii) The equations of State II [t_1 to t_2] are: -

$$v_{C1a} = V_S + I_o T_S \omega_0 Z_0 \quad (2.6)$$

$$v_{C1b} = 2V_S + \frac{I_o T_S \omega_0 Z_0}{2} \quad (2.7)$$

$$i_{Lr} = 0 \quad (2.8)$$

(iii) The equations of State III [t_2 to t_3] are: -

$$v_{C1a} = V_S + \frac{3}{4} I_o T_S \omega_0 Z_0 \cos \omega_0 (t - t_2) \quad (2.9)$$

$$i_{Lr} = -\frac{3}{4} I_o T_S \omega_0 \sin \omega_0 (t - t_2) \quad (2.10)$$

$$v_{C1b} = 2V_S + \frac{3I_o T_S \omega_0 Z_0}{4} \cos \omega_0 (t - t_2) \quad (2.11)$$

(iv) The equations of State IV [t_3 to t_4] are: -

$$v_{C1a} = V_S - I_o T_S \omega_0 Z_0 \quad (2.12)$$

$$v_{C1b} = 2V_S - \frac{I_o T_S \omega_0 Z_0}{2} \quad (2.13)$$

$$i_{Lr} = 0 \quad (2.14)$$

2.2.3. Simulation Results

The simulation result of the triple-mode step-up converter is shown in Fig. 2.3. The result is provide that the input voltage is 40V, output power is 100W, switching frequency is 200kHz, C_{1a} and C_{1b} are 0.22 μ F, L_r is 1 μ H and C_{2a} is 50 μ F. Further to the simulation result, assuming the output capacitor, C_{2b} , is very large to maintain constant output voltage. As the result, the capacitance of C_{1a} is equal to that of C_{1b} such that the circuit has no power loss in the circuit.

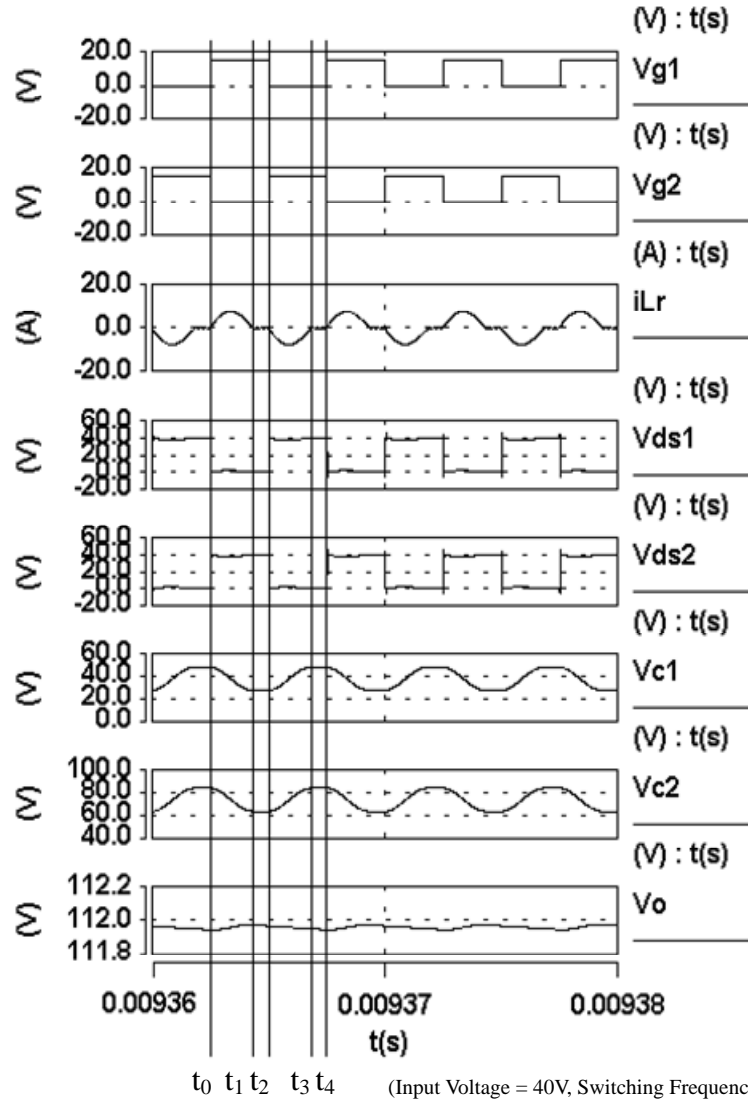


Fig. 2.3 Simulation waveforms of triple mode switched-capacitor resonant converter

Table 2.1 Variable of the simulation waveforms

V_{g1}	Switch S_1 gate signal	V_{ds2}	Voltage between the drain and source of switch S_2 (FET)
V_{g2}	Switch S_2 gate signal	V_{c1}	Voltage of the capacitor C_{1a}
i_{Lr}	Current of resonant inductor L_r	V_{c2}	Voltage of the capacitor C_{2a}
V_{ds1}	Voltage between the drain and source of switch S_1 (FET)	V_o	Output Voltage

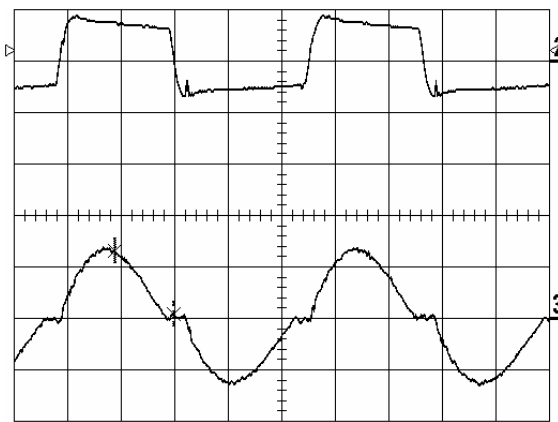
2.2.4. Experimental Results

In this chapter, the triple-mode step-up resonant converter shown in Fig. 2.1(b) and 2.3 has been tested. The circuit is very similar to the circuit diagram that shown in Fig. 2.1(b) and 2.3 except that a filtering capacitor C_{in} was added to eliminate effects from the inductance of the conduction line between the power source and the input of the converter. For output voltage ripple less than 2%, specification of prototype of the circuit is shown in Table 2.2.

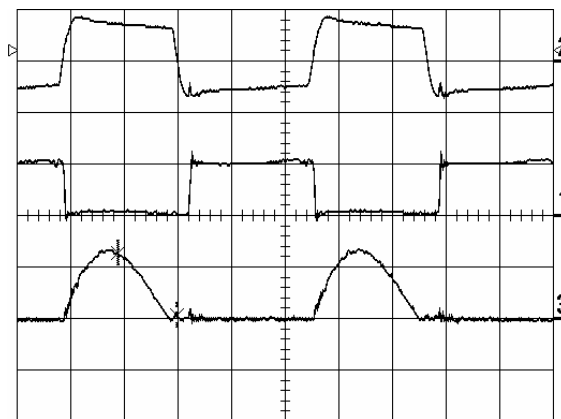
Table 2.2 Specification of Prototype of Triple-mode Converters

Descriptions	Model Numbers	Values	Units
Input Voltage	/	40	V
Expected Output Voltage	/	120	V
Switching Frequency	/	215	kHz
Output Power	/	10-90	W
S_1 and S_2 (Switching Device)	IRF530	/	/
D_{1a} , D_{1b} , D_{2a} and D_{2b} (Diode)	MBR10100	/	/
C_{1a} , C_{1b}	/	0.22	μ F
C_{2a}	/	50	μ F
C_{2b}	/	100	μ F
L_r	/	1	μ H

Since the main power flows through both C_{1a} and C_{2b} in the resonant state, the equivalent series resistance of these capacitors should be very low. High ESR may lead to high power loss and high temperature of the capacitors which may exceed the rated temperature of the capacitors. For this reason, polyester capacitors were chosen for these switched-capacitors and the experimental result of prototype triple-mode zero-current quasi-resonant switched-capacitor converter shown in Fig. 2.4.



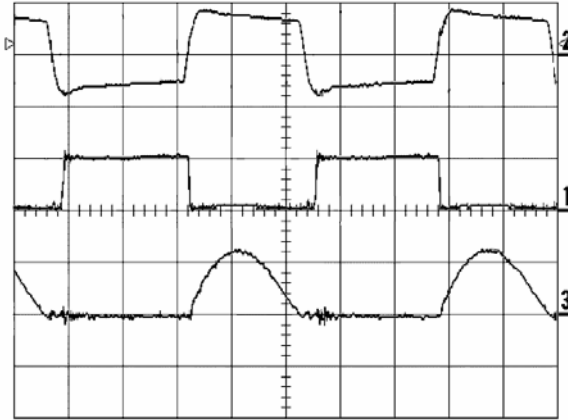
(a) Upper trace: Gate signal of S_1 , 20V/div, Lower trace: I_L , 5A/div



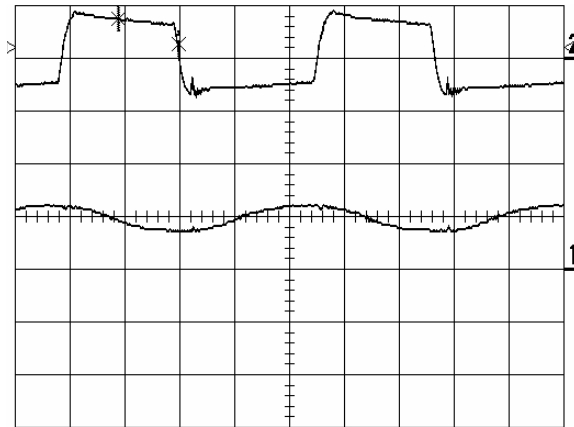
(b) Upper trace: Gate signal of S_1 , 20V/div, Middle trace: V_{ds} of S_1 , 40V/div

Lower trace: S_1 current, 5A/div

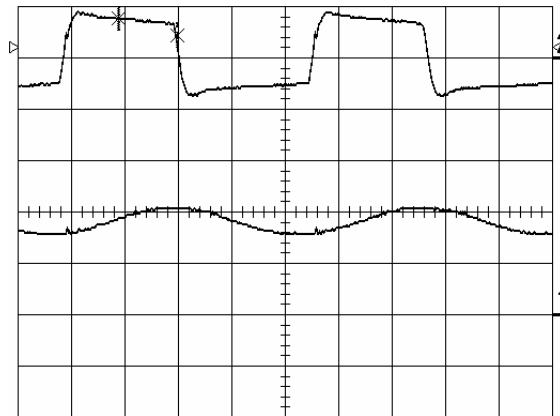
Fig. 2.4 Measured waveforms of triple mode switched-capacitor resonant converter



(c) Upper trace: Gate signal of S_2 , 20V/div, Middle trace: V_{ds} of S_2 , 40V/div
Lower trace: S_2 current, 5A/div

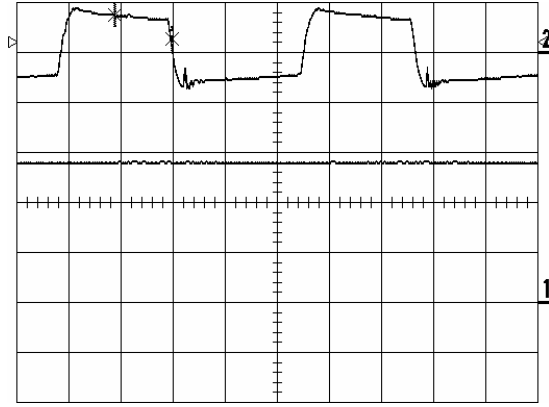


(d) Upper trace: Gate signal of S_1 , 20V/div, Lower trace: V_{C1a} , 40V/div



(e) Upper trace: Gate signal of S_2 , 20V/div, Lower trace: V_{C1b} , 40V/div

Fig. 2.4 Measured waveforms of triple mode switched-capacitor resonant converter



(f) Upper trace: Gate signal of S_1 , 20V/div,

Lower trace: Output Voltage, 40V/div

Time base = $5\mu\text{s}/\text{div}$ for (a) to (e)

Fig. 2.4 Measured waveforms of triple mode switched-capacitor resonant converter

Measured waveforms of the triple-mode step-down zero-current switching quasi-resonant converter operating with 90W output power are shown in Fig. 2.4. From both Fig. 2.4(a) and (b), they show that the switching devices S_1 and S_2 are zero-current switching during switching on and off in a sinusoidal manner. The Fig. 2.4(d) and (e) shows the voltage of C_{1a} and C_{1b} . It can be seen that there is a dc component of V_s and $2V_s$ on the voltages of C_{1a} and C_{1b} respectively. The resonant component is small as expected. The amplitude of the resonant voltage and current have been examined and confirmed that they agree with the equations derived, with a small deviation because of the energy loss in the circuit. The waveforms agree with the simulation as shown in Fig 2.3 and the graph of characteristic of efficiency shown in Fig. 2.5 and Table 2.3, it can be seen that the efficiency of the converter is around 90% at 90W power output.

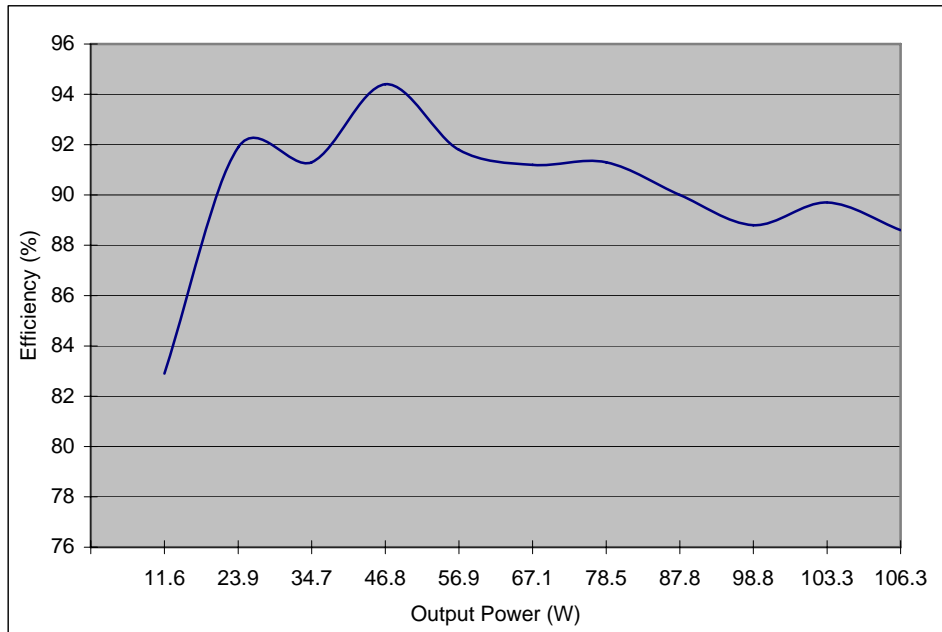


Fig. 2.5 Measured efficiency and output power of the triple mode switched-capacitor resonant converter

Table 2.3 Measured efficiency, input and output value of the triple mode switched-capacitor resonant converter

Input			Output			Efficiency
Volt(V)	I(A)	P(W)	Volt(V)	I(A)	P(W)	%
40	0.35	14	120.9	0.1	11.6	82.9
40	0.65	26	118.4	0.2	23.9	91.9
40	0.95	38	116.5	0.3	34.7	91.3
40	1.24	49.6	115.8	0.4	46.8	94.4
40	1.55	62	113.8	0.5	56.9	91.8
40	1.84	73.6	112.6	0.6	67.1	91.2
40	2.15	86	111.8	0.7	78.5	91.3
40	2.44	97.6	110.1	0.8	87.8	90
40	2.78	111.2	109.3	0.9	98.8	88.8
40	2.88	115.2	108.5	0.95	103.3	89.7
40	3	120	107.4	1	106.3	88.6

2.3. Discussion

The design of step-up zero-current quasi-resonant switched-capacitor converters resonant is very simple. The efficiency of the converters is high referring to the experiment result. Hence, the high efficiency is obtained by the quasi-resonant zero-current switching. In the conventional switched-capacitor converters the output voltage cannot be regulated or controlled by controlling the charging and discharging periods of the switched-capacitor. But the both zero-current quasi-resonant switched-capacitors converter circuits have to be control the charged and discharged of the switched-capacitor in fixed periods, half resonant period for zero-current switching. The zero-current switching technique applying in the quasi-resonant switched-capacitors converter reduces the switching loss of switching devices greatly. Unfortunately, the drain-to-source junction capacitors of the transistors contain the switching loss. The switching loss is directly proportional to the switching frequency. For higher fraction and higher multiplication conversion ratio of the both step-up and step-down resonant switched-capacitor converters, more diodes are needed for routing the charging and discharging current. Efficiency of the converters will be lower because of forward voltage of the diodes.

In practical, schottky diodes may be used for this application. Their forward voltage is from 0.5V to 0.8V, depending on their ratings. The higher number of diodes leads to higher conduction loss due to their forward voltage. It also leads to the higher voltage drop of the output voltage. When higher

multiplication of the voltage conversion ratio is obtained, number of stages is higher. Number of filtering capacitors is also higher. The size of the converter will be higher because not only the total size of the diodes is higher but also that of the capacitors is higher. However, in practical, the filtering capacitors are electrolytic capacitors. They have high capacitance values with small size and light weight. The total size of the capacitors will not much increases.

Because of the discontinuous discharging current of the switched-capacitors to the load, comparing with a continuous mode traditional SMPS, the capacitance value of the output capacitor is higher. In practical, the output capacitor is an electrolytic capacitor. The size of the capacitor is slightly bigger than that in a traditional SMPS.

2.4. Summary

The switched-capacitor circuits of zero-current switching quasi-resonant step-down converter are introduced in this chapter. The circuit of zero-current switching quasi-resonant step-up converter is operating under zero-current switching and there is only a very small inductor providing resonance in each circuit and no large inductor is needed for energy storage. Thus, the inherent shortcoming of high current stress in transistor has been eliminated and also the number of transistors for switching has been reducing to two. The equations and analysis of the triple-mode zero-current switching quasi-resonant step-up converter circuits have been provided and presented. The computer simulation and the experiments result of triple-mode switched-capacitor converters with 100W prototype had been tested and analysis. Besides, the result shown all switching transistors has been operate under zero-current switching condition for all transistors. Both switching loss and EMI have been reduced. High efficiency can then be obtained. From the experiment, it shows that the efficiency of the converter can be around 90%. Also, current spike problem does not exist in this circuit.

Chapter 3 Principles of Power Factor Correction Techniques in Zero-current Switching Quasi-resonant Switched-capacitor conversion

3.1 Introduction

Nowadays, the PFC techniques are widely applied in many conventional converters to shape the converter input current waveform to nearly sinusoidal and in phase with the input supply voltage in order to improve the power factor and efficiency of the conventional converters.

In this chapter, the new concept of the PFC techniques applying zero-current switching quasi-resonant switched-capacitor converters is introduced. The study also includes the operation principle and voltage control frequency technique.

3.2 Concept of Power Factor Correction Techniques in Zero-current Switching Quasi-resonant Switched-capacitor Converters

The operation principle, different states, equivalent circuits and mathematical analysis of step-up and step-down PFC zero-current switching quasi-resonant switched-capacitor DC-DC converters are already discussed and analysed in chapter 2. The advantage of zero-current switching quasi-resonant switched-capacitor converters is to provide high efficiency of fixed conversion

ratio and overcome the low efficiency. Besides, switching loss in classical switched-capacitor converters was improved. The energy processing for resonant switched-capacitor is not required to process the total energy stored in the converters but only a small portion whereas the classical switched-mode power supplies (SMPS) are required to have the total or a large portion of energy stored in the reactive components processed [3.1]. Therefore the power efficiency cannot be very high in the classical SMPS. The method to apply the PFC in switched-mode power converters such as Buck, Boost and Buck-boost has been reported by many researchers. It is proposed to apply the resonant switched-capacitor concept for use in PFC. Therefore the main advantage of the resonant switched-capacitor conversion can be integrated with the PFC.

A new concept of voltage control frequency technique has been developed to control the switching devices. It is because the conventional switched-capacitor converter is drawing a pulsating input current. In this case, the power factor is lower and the harmonic is large. This technique is to control the switching frequency by the reference input voltage signal to overcome the shortcoming and achieve the nearly sinusoids input current. This PFC controller can generate the variable switching frequency similar to the VCO to drive the switching device of the converter. The switching frequency range of the VCO is preset at around 100 kHz to 200 kHz depending on the reference sine-wave input voltage amplitude. So, the VCO switching frequency will equal to 100 kHz when reference sine-wave input voltage amplitude is equal to zero voltage. Such that, the VCO output frequency is proportional to the reference sine wave input voltage amplitude. In the converter all components

are set as 200 kHz resonant frequencies. Properly controlling the transistors S_1 and S_2 , all the currents resonate from zero and finish at zero values. Therefore zero-current switching can be attained. At low switching frequency periods the reference sine wave input voltage amplitude and current draws by the converter are also lower. In this case, the input current of the converter is lower otherwise the input current is rise against the high reference sine wave input voltage amplitude and high switching frequency generate by VCO. As the result, the zero-current switching quasi-resonant switched-capacitor converters will draw an input current in nearly sinusoidal and in phase with the input supply voltage. On the other hand, the zero-current switching capability can also be maintained.

3.3 Principle of Power Factor Correction Techniques in Zero-current Switching Quasi-resonant Switched-capacitor Converters

The zero-current switching quasi-resonant switched-capacitor converters operate under high switching frequency. This new control circuit strategy uses 50Hz input supply AC voltage amplitude as a reference signal to control the switching frequency of the converters. The operation block diagram is shown in Fig. 3.1.

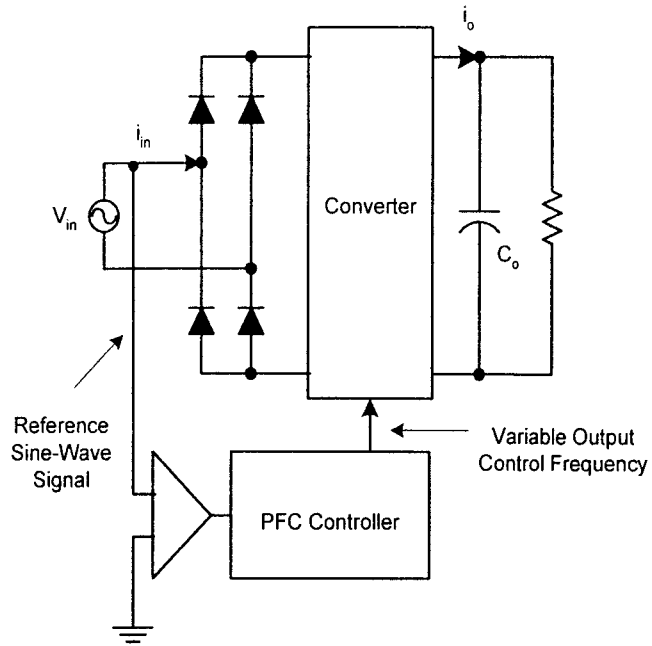


Fig. 3.1 Principle control block diagram

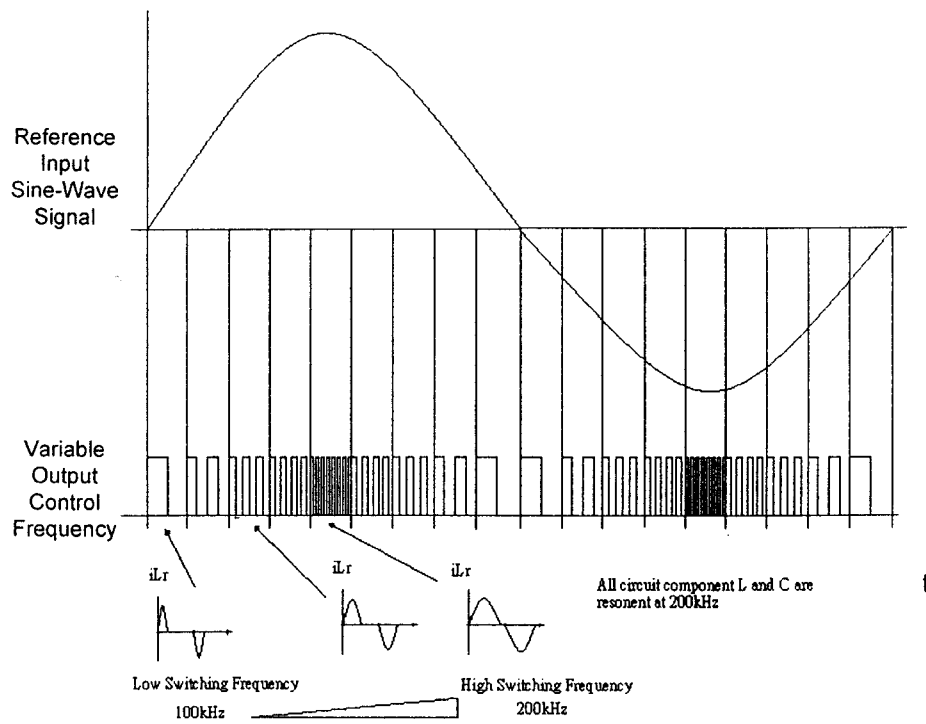


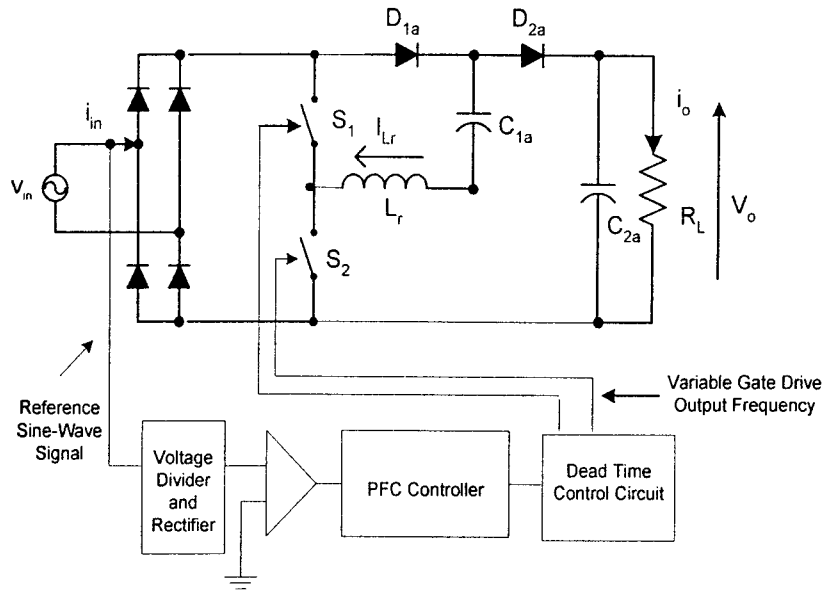
Fig. 3.2 Variable output frequency waveform of the PFC controller

This controller circuit output frequency is similar to the voltage control oscillator (VCO) shown in Fig 3.2. At initial state, the reference sine-wave signal voltage is equal to zero. At the same time the PFC controller start to oscillate at a low frequency, which is preset at 80 - 100 kHz as shown on Fig. 3.2. Meanwhile, the input AC voltage increases from zero in sinusoidal manner and the PFC controller will increase the output frequency to drive the switching devices according to the 50Hz input voltage amplitude.

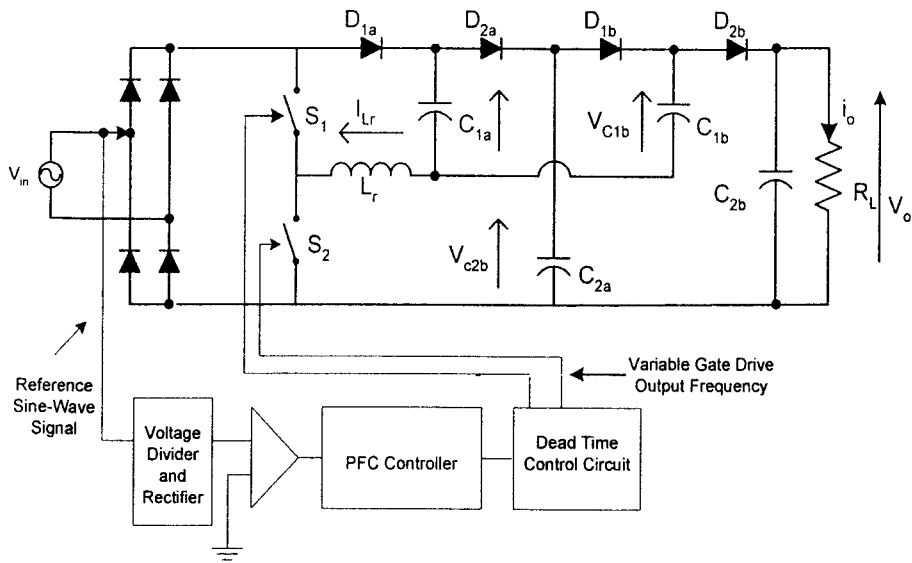
This PFC controller continues to drive the switching devices and the output frequency varies according to amplitudes of input reference sin-wave voltage. Assuming that each time period is fixed, Fig. 3.2 shows the frequency and reference sine-wave relationship accordingly.

In this approach, the input current amplitude of the converter is depending on the reference voltage amplitude and switching frequency. For example, the lower reference voltage amplitude will generate the low output switching frequency. In this case, the current draw from the input will lower. Otherwise, the high input current will obtain during the reference voltage at peak value. The detail input current waveform as show in Fig 3.3.

The proposed PFC zero-current switching quasi-resonant switched-capacitor AD-DC converters can be developed into the step-up, step-down and inverting mode as shown in Fig 3.3, 3.4 and 3.5 respectively.

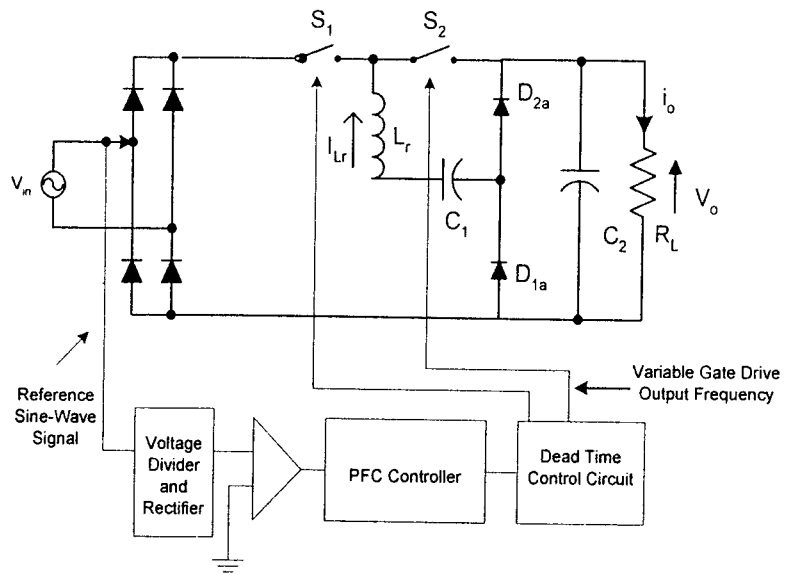


(a) Step-up double mode

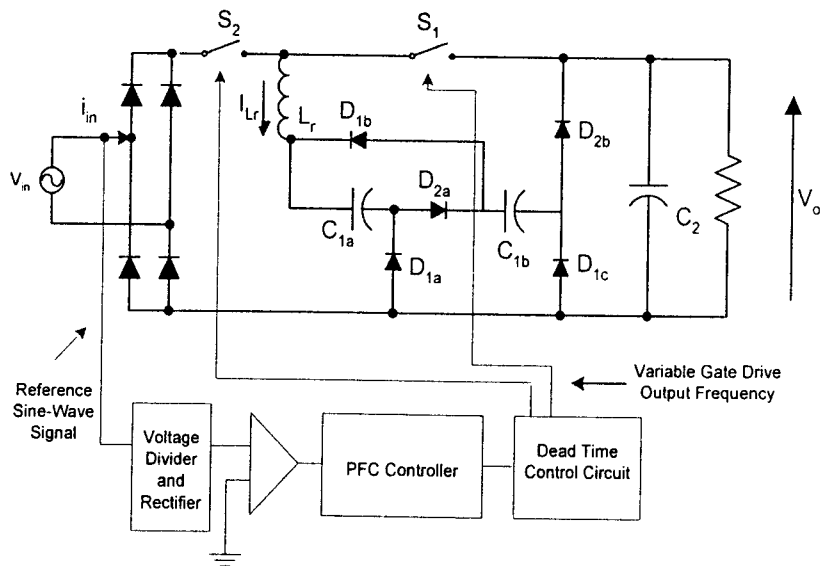


(b) Step-up triple mode

Fig 3.3 Step-up PFC circuit

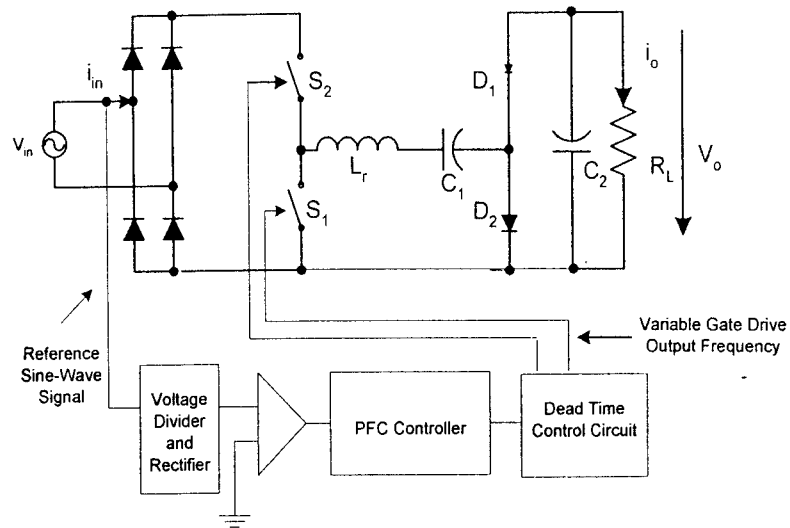


(a) Step-down $1/2$ mode

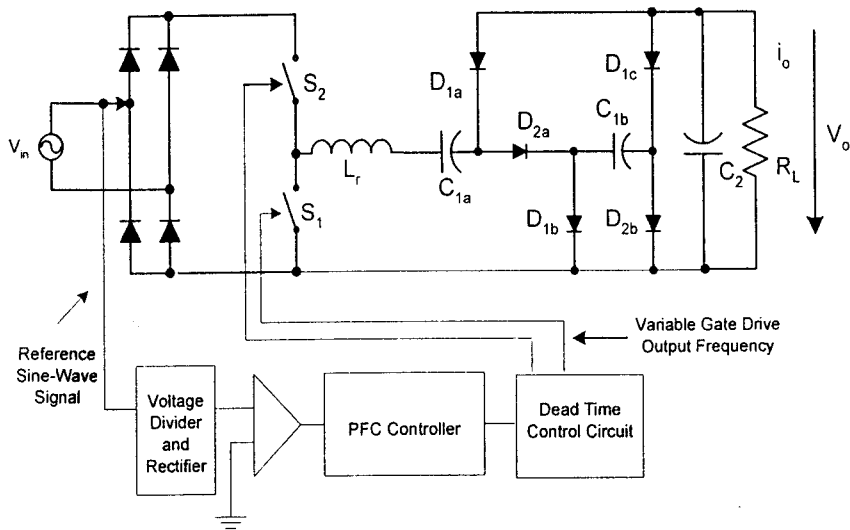


(b) Step-down $1/3$ mode

Fig 3.4 Non-Inverting Step-down PFC circuit



(a) *Inverting unity mode*



(b) *Inverting half-mode*

Fig 3.5 *Inverting mode PFC circuit*

3.4 Family of Quasi-Resonant Switched Capacitor PFC circuits

The non-inverting step up version as shown in Fig 3.3 is simply changed the input stage from a DC voltage into an AC source. The transistors S_1 and S_2 are also switched alternative manner with 50% duty ratio of a switching period. The frequency of switching period is regulated with the input 50Hz amplitude. For the step-up circuit, the input current is a summation of current through S_1 and S_2 . It is bipolar before the bridge rectifier and is unipolar after the bridge rectifier. For the step-down circuit as shown in Fig 3.4, the input current before and after the bridge rectifier is given by the current through S_1 . During S_2 conducting, its current does not pass through bridge rectifier and therefore only half of the quasi-resonant cycle is reflected in the bridge rectifier.

For the step-down inverting circuit as shown in Fig 3.5, the input current is defined by the current through S_2 . During S_1 conducting, its current only flow to the right hand side of the circuit and does not flow through the input. Therefore the input current is dependent on the half of the resonant current of L_r .

3.5 DC/DC Converter Techniques for Shaping the Converters

Input Current

The separately controlled DC/DC converters are sufficient for producing a regulated dc output stack voltage of the designed PFC converters and shaping the input source current [3.4]. Fig. 3.6 shows the proposed PFC converter that is constructed by two converter circuits (two complete converters).

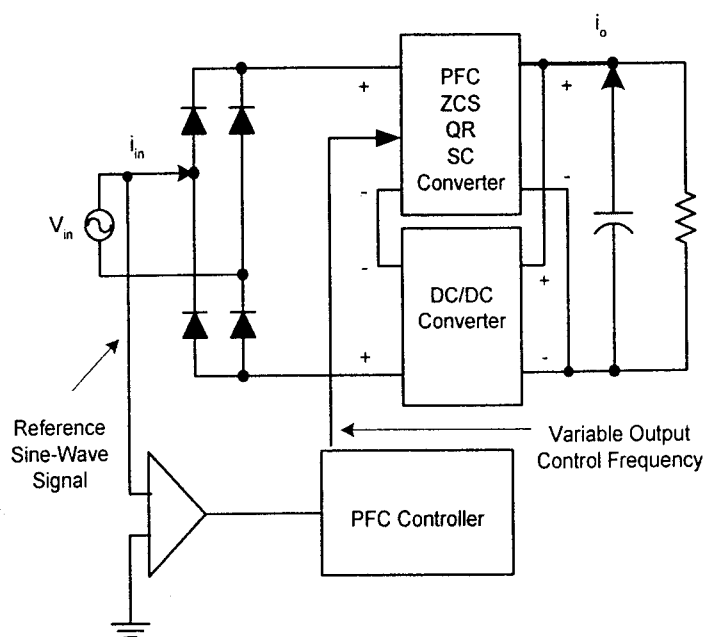


Fig 3.6 PFC circuit with shaping DC/DC converter

First of all, we observe that the resonant tanks formed by L_r and C_1 did not resonate when the input voltage is smaller than certain value shown in Fig. 3.3(b). This is mainly because the diodes D_{2a} and D_{2b} only conduct under forward bias. When the input voltage is small, the diodes are under reverse bias and the resonance cannot be excited. The problem can be solved if one stacks up a sufficiently large dc voltage over the ac input voltage before feeding into a proposed step-up PFC converter.

Our next step is to generate a stack-up voltage. Obviously, we need a second DC/DC converter, which converts a stack-up voltage from the output voltage. This gives the basic configuration shown in Fig. 3.7, which is simply a series connection of step-up PFC converter and the stack-up DC/DC converters. The step-up DC/DC converter must be capable of converting a variable dc voltage to a fixed dc voltage. This circuit connection achieves unity power factor and shaping input current.

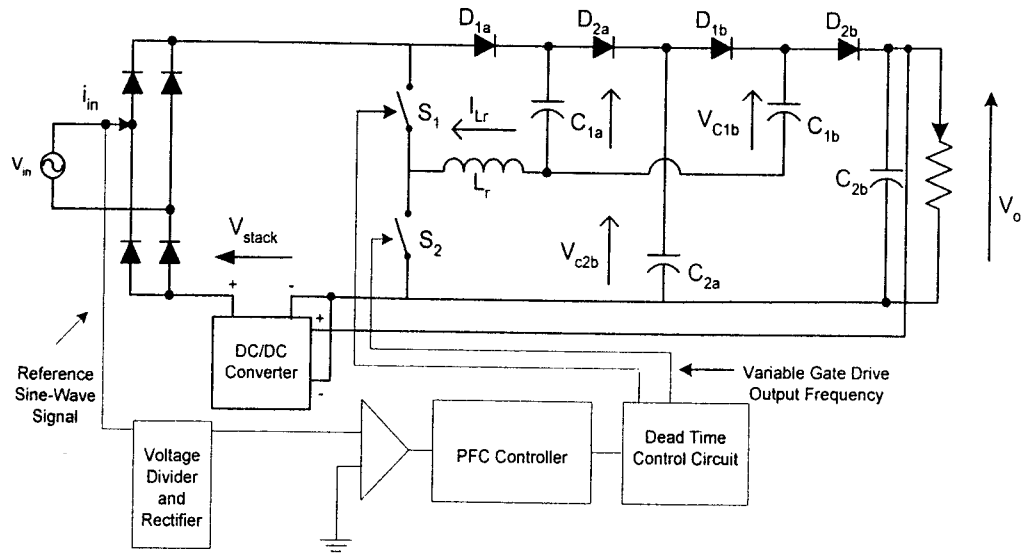


Fig 3.7 Step-up PFC circuit with shaping DC/DC converter

Let us define the gain of the switched-capacitor converter be G_1 and the gain of the DC/DC converter be G_2 . Hence,

$$(v_{in} - V_{stack})G_1 = V_o \quad (3.1)$$

$$V_o G_2 = V_{stack} \quad (3.2)$$

$$\frac{V_o}{v_{in}} = \frac{G_1}{1 - G_1 G_2} \quad \text{for } v_{in} \neq 0 \quad (3.3)$$

where $v_{in} = V_{in} \sin \omega t$

At $v_{in} = 0$ which is the time at zero current of the sine wave,

$$G_1 = \frac{V_o}{V_{stack}} \quad \text{and } G_1 G_2 = 1 \quad (3.4)$$

For ideal power flow and assume the input current is:

$$i_{in} = I_{in} \sin \omega t$$

The input and output power balance gives:

$$P_o = \frac{V_{in} I_{in}}{2} = V_o I_o \quad (3.5)$$

The power handling for the switched-capacitor converter is:

$$P_1 = \int_0^{T_s} (V_{in} \sin \omega t + V_{stack}) I_{in} \sin \omega t \, dt = P_o \left(1 + \frac{4V_{stack}}{\pi V_{in}} \right) \quad (3.6)$$

The power handling of the DC/DC converter is:

$$P_2 = \int_0^{T_s} (V_{stack}) I_{in} \sin \omega t \, dt = P_o \left(\frac{4V_{stack}}{\pi V_{in}} \right) \quad (3.7)$$

It can be seen that the power processing by the DC/DC converter is zero and in ideal case, there is no loss by the DC/DC converter. It is just used to help the shape the switching profile of the power factor correction circuit.

The amplitude of V_{stack} is not necessary to be higher than V_{in} . However, it is better to make them close to each other in order to make the current shaping to be more sinusoidal. Because of the regulation of the input current depends on the input voltage, the resultant voltage goes to the switched-capacitor converter is a sum of sine wave and a DC that is just a level shift to more positive and hence the current shaping near the zero-crossing is improved.

3.6 Summary

In this chapter, the zero-current switching quasi-resonant switched-capacitor is introduced for use in AC-DC converters. The proposed circuit is able to perform power factor correction and is regarded as a method that has been used for SMPS. Discontinuous mode is used for the current control. This is also the only method that is feasible for the zero-current switching quasi-resonant switched-capacitor because its current is also discontinuous. The current shaping is realised by the frequency control such that near the zero-crossing of the 50Hz sine input voltage, a low switching frequency is applied whereas for the peak and trough of the input sine wave, high switching frequency is applied. This control circuit is realised by the voltage control oscillator (VCO). The main advantages of this circuit are very simple and maintaining the zero-current switching of the switched-capacitor converters. Of course, the design rule of thumb is that the maximum switching frequency generated by the VCO is set at slightly lower than the resonant frequency of the switched-capacitor resonant tank in order to ensure zero-current switching can be fulfilled all the time. The separately controlled stack-up DC/DC converters are sufficient for producing a regulated DC output voltage of the designed PFC converters and shaping the input source current. The detailed design and analysis is presented in next chapter.

Chapter 4 Mathematical Analysis of the Power Factor Correction Zero-current Switching Switched-capacitor AC-DC Converters

4.1 Introduction

The equations governing the switched-capacitor converter under AC-DC PFC condition is different from the DC-DC conversion as shown in Chapter 2. For the present development, the AC-DC converter has an input of sine wave and there exists three frequencies in the circuit. One is the resonant tank frequency, switching frequency and the AC source input frequency. The resonant frequency and the switching frequency are very close in quantity whereas the AC source frequency is very low as compared to the switching frequency. Therefore in each switching cycle, the input AC voltage can be considered as constant. The original frequency as shown in Chapter 2 and appendix for the basic DC-DC counterpart is reformatted in order to meet the AC-DC conversion concept. In this chapter, the mathematical analysis, design criteria and generalised analysis will be presented.

4.2 Initial Analysis On Single Stage Step-up PFC Circuit

4.2.1 State Equations of the Step-up Circuit

The application of the ZCS switched-capacitor converter is firstly tested for the mathematical analysis based on the single stage circuit, the non-inverting double mode circuit. The circuit is given in Fig 4.1. The following assumption is used for the analysis.

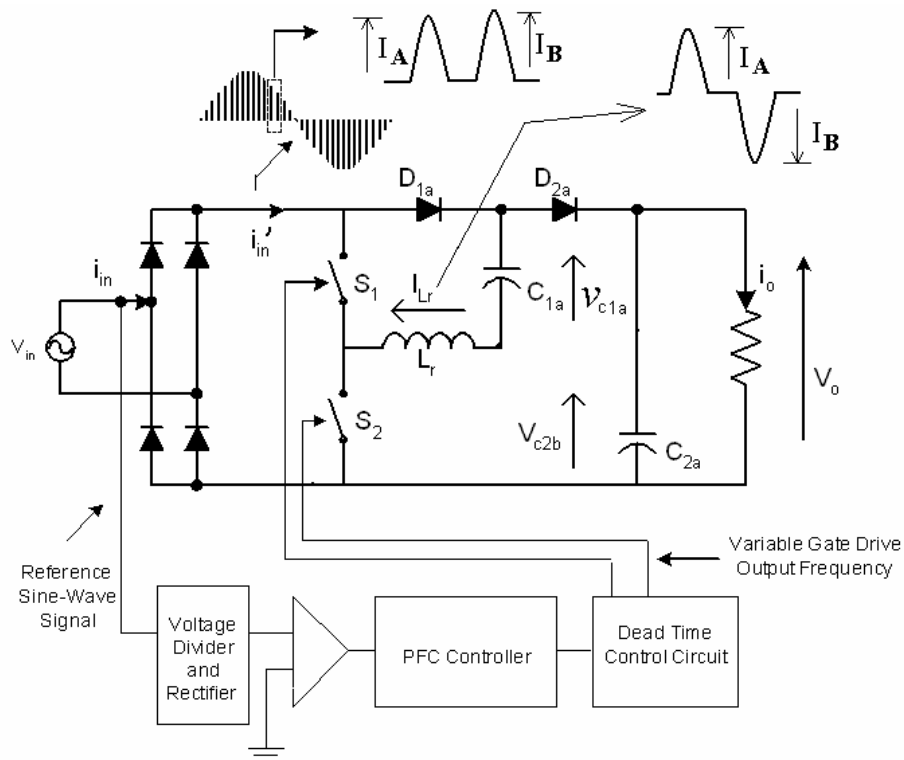


Fig 4.1 Schematic of the power factor correction circuit using double mode step-up version

- a) The output capacitor connected to the load R_L is large and its voltage is assumed to be constant. Therefore for double mode circuit, C_{2a} is large.
- b) There are no losses in the switching device (Transistor and diode).
- c) The ESR for the resonant inductor L_r and resonant capacitor C_{1a} , are small.
- d) The switching period is small when compared to the input period of the AC source.

The switching period again can be divided into four stages of operation as shown in Fig 4.2.

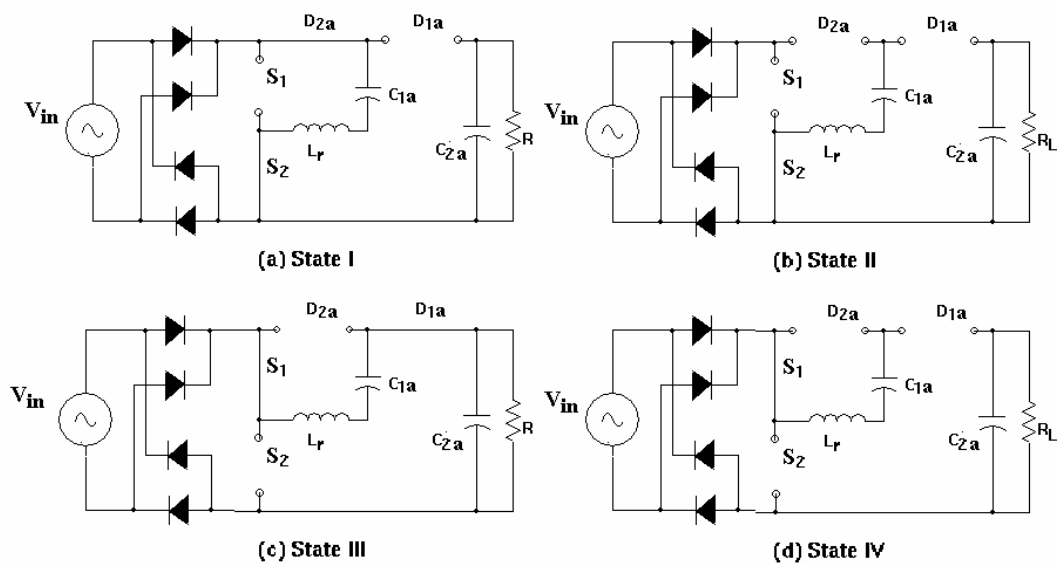


Fig 4.2 Equivalent circuit during 4 stages of operation

(i) *State I* [t_0 - t_1],

Transistor S_2 is turned on, the resonant tank L_r and C_{1a} starts to resonate as the same manner as the DC-DC resonant switched-capacitor converter (See Chapter 2 or [4.1]). The state equations are given as below: -

$$v_{in} = L_r \frac{di_{Lr}}{dt} + v_{C1a} \quad (4.1)$$

$$i_{Lr} = C_{1a} \frac{dv_{C1a}}{dt} \quad (4.2)$$

$$\text{where } v_{in} = V_{in} \sin \omega t \quad (4.3)$$

and ω is the AC source frequency

The solutions are

$$v_{C1a} = V_{in} \sin \omega t - I_A Z \cos \omega_o t \quad (4.4)$$

$$i_{Lr} = I_A \sin \omega_o t \quad (4.5)$$

$$\text{where } Z = \sqrt{\frac{L_r}{C_{1a}}} \quad (4.6)$$

$$\omega_o = \sqrt{\frac{1}{L_r C_{1a}}} = \frac{2\pi}{T_o} \quad (4.7)$$

(ii) *State II* [t_1 - t_2],

At $t = t_1$ to t_2 , the resonant current i_{Lr} and voltage v_{C1a} remain unchanged: -

$$v_{C1a} = V_{in} \sin \omega t + I_A Z \quad (4.8)$$

$$i_{Lr} = 0 \quad (4.9)$$

(ii) *State III* [t_2 - t_3],

Transistor S1 is turned on, the resonant tank formed by L_r and C_{1a} starts to resonate in the same manner as the DC-DC resonant switched-capacitor converter (See Chapter 2 or [4.1]). The state equations are: -

$$v_{in} = V_o - L_r \frac{di_{Lr}}{dt} - v_{C1a} \quad (4.10)$$

$$i_{Lr} = C_{1a} \frac{dv_{C1a}}{dt} \quad (4.11)$$

The solutions are

$$v_{C1a} = (V_o - V_{in} \sin \omega t) + I_B Z \cos \omega_o (t - t_2) \quad (4.12)$$

$$i_{Lr} = -I_B \sin \omega_o (t - t_2) \quad (4.13)$$

(iv) *State IV* [t_3 - t_4],

At $t=t_3$ to t_4 , the resonant current i_{Lr} and voltage v_{c1a} remain unchanged:

$$v_{C1a} = (V_o - V_{in} \sin \omega t) - I_B Z \quad (4.14)$$

$$i_{Lr} = 0 \quad (4.15)$$

I_A and I_B are the amplitude of the resonant current in the State I and II respectively.

4.2.2 Continuity Analysis and Energy Equation

Eqns (4.1) to (4.13) cannot be solved as described in Chapter 2 or [4.2]. It is because t_4 in State IV and t_0 at State I are not continuous mode. However, t_2 in State II and t_2 at State III are operating in continuous mode. Eqns (4.8) and (4.12) can therefore be solved as follows: -

$$v_{C1a} |_{t=t_2} = (V_o - V_{in} \sin \omega t) + I_B Z = V_{in} \sin \omega t + Z I_A \quad (4.16)$$

It follows that: -

$$I_B - I_A = \frac{2V_{in} \sin \omega t - V_o}{Z} \quad (4.17)$$

Another condition is based on the current of i_{in} . i_{Lr} is formed by i_{in}' and the train of inductor current, i_{Lr} . Therefore, the average current of i_{Lr} appeared at i_{in}' is then given as follows: -

$$\frac{I_A + I_B}{\pi} \frac{2T_o}{T_s} k = I_{in} \sin \omega t \quad (4.18)$$

where k is a VCO variable and is a function of t . I_{in} is the amplitude of i_{in} . It represents the conversion of the voltage, V_{in} , to switching frequency, which use to drive the S_1 and S_2 . T_o and T_s are the period of resonant tank as shown in Eqn (4.7) and period of switching frequency.

Another condition is based on the energy conversion. The input and output energy is conserved and hence: -

$$I_{in} = \frac{2V_o I_o}{V_{in}} \quad (4.19)$$

Eqns (4.17-4.19) can be solved and give: -

$$I_B = \frac{1}{2} \left(\frac{I_{in} \sin \omega t \pi T_S}{2T_o k} + \frac{2V_{in} \sin \omega t - V_o}{Z} \right) \quad (4.20)$$

It could also be noted that the voltage rating of the transistors S_1 and S_2 are equal to source voltage of V_{in} . The voltage ratings of all the diodes are also approximately equal to V_{in} .

4.3 Analysis On Triple Step-up PFC Circuit

4.3.1 State Equations of the Step-up Circuit

The triple mode circuit is analysed here. There are 4 operation stages in the double mode circuit. The equivalent circuit of each stage is similar to Fig 4.2. The circuit is shown in Fig 4.3. The operation in each state is given as below: -

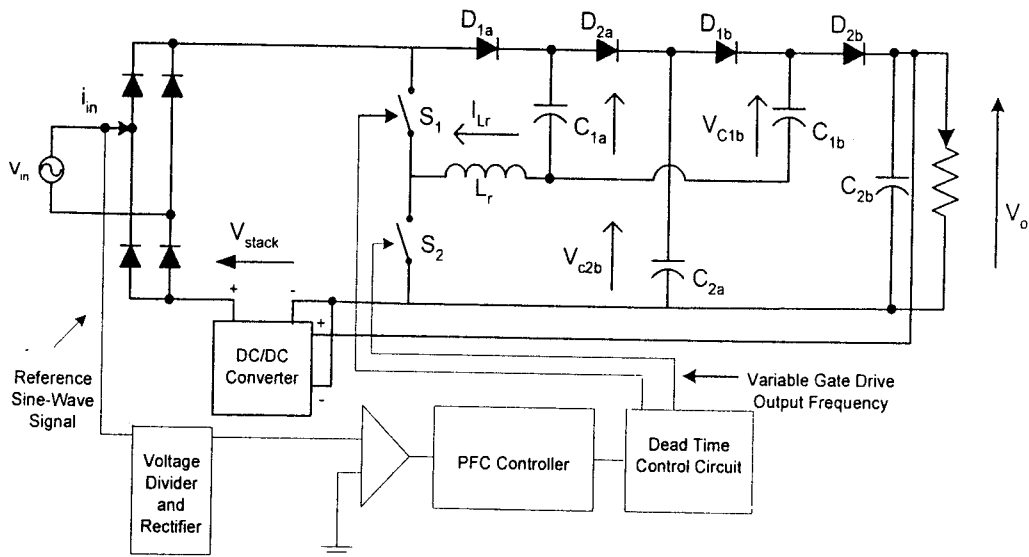


Fig 4.3 Circuit of the step-up triple circuit with shaping DC/DC converter

(i) State I [t_0-t_1]

Transistor S_2 is turned on, the resonant tank L_r and C_{1a} start to resonate. The operation principle of the step-up triple circuit is similar to that of the DC-DC resonant switched-capacitor converter (See Chapter 2 or [4.1]).

The operation state equations are shown as follows: -

$$v_{in} = L_r \frac{di_{Lr}}{dt} + v_{C1a} + V_{stack} \quad (4.21)$$

$$i_{Lr} = C_{1a} \frac{dv_{C1a}}{dt} \quad (4.22)$$

$$v_{C1b} = v_{C2a} - L_r \frac{di_{Lr}}{dt} \quad (4.23)$$

The solutions are: -

$$v_{C1a} = V_{in} \sin \omega t - V_{stack} - I_A Z \cos \omega_o t \quad (4.24)$$

$$i_{Lr} = I_A \sin \omega_o t \quad (4.25)$$

$$v_{C1b} = v_{c2a} - I_A Z \cos \omega_o t \quad (4.26)$$

$$\text{where } Z = \sqrt{\frac{L_r}{2C_1}} \quad (4.27)$$

$$\omega_o = \sqrt{\frac{1}{2L_r C_1}} = \frac{2\pi}{T_o} \quad (4.28)$$

C_{1a} and C_{1b} are assumed to be the same and are equal to C_1

(ii) *State II* [t_1 - t_2]

At $t = t_1$ to t_2 , the resonant current i_{Lr} , voltage v_{c1a} and v_{c1b} remain unchanged:-

$$v_{C1a} = V_{in} \sin \omega t - V_{stack} + I_A Z \quad (4.29)$$

$$i_{Lr} = 0 \quad (4.30)$$

$$v_{C1b} = v_{c2a} + I_A Z \quad (4.31)$$

(iii) *State III* [t_2 - t_3],

Transistor S_1 is turned on, the resonant tank is formed by L_r , C_{1a} and C_{1b} start to resonate. The operation principle of the step-up triple circuit is similar to that of the DC-DC resonant switched-capacitor converter (See [4.2]). The state equations are given as follows: -

$$v_{in} - V_{stack} = v_{C2a} - L_r \frac{di_{Lr}}{dt} - v_{C1a} \quad (4.32)$$

$$i_{Lr} = C_{1a} \frac{dv_{C1a}}{dt} + C_{1b} \frac{dv_{C1b}}{dt} \quad (4.33)$$

$$v_{in} = V_o - L_r \frac{di_{Lr}}{dt} - v_{C1b} \quad (4.34)$$

The solutions are: -

$$v_{C1a} = (v_{C2a} - V_{in} \sin \omega t + V_{stack}) + I_B Z \cos \omega_o (t - t_2) \quad (4.35)$$

$$i_{Lr} = -I_B \sin \omega_o (t - t_2) \quad (4.36)$$

$$v_{C1b} = (V_o - V_{in} \sin \omega t) + I_B Z \cos \omega_o (t - t_2) \quad (4.37)$$

(iv) *State IV* [t_3 - t_4],

At $t = t_3$ to t_4 , the resonant current i_{Lr} , voltages v_{C1a} and v_{C1b} remain unchanged: -

$$v_{C1a} = (V_o - V_{in} \sin \omega t + V_{stack}) - I_B Z \quad (4.38)$$

$$i_{Lr} = 0 \quad (4.39)$$

$$v_{C1b} = (V_o - V_{in} \sin \omega t + V_{stack}) - I_B Z \quad (4.40)$$

Again, I_A and I_B are the amplitude of the resonant current during the State I and II respectively.

4.3.2 Continuity Analysis and Energy Equation

Eqns (4.21) to (4.40) cannot be solved like in [4.1] and [4.2]. It is because t_4 in State IV and t_0 in State I are not operated in continuous mode. However, t_2 in State II and III are also operated in continuous mode. Therefore, Eqns (4.29), (4.31), (4.32) and (4.34) can then be solved. It is noted that V_{C2a} is not a constant voltage. The Capacitor C_{2a} is not large and the voltage of C_{2a} includes the component of AC source frequency and DC voltage. The detail is given as follows: -

$$v_{C1a} |_{t=t_2} = V_{in} \sin \omega t - V_{stack} + ZI_A = v_{C2a} - V_{in} \sin \omega t + V_{stack} - ZI_B \quad (4.41)$$

$$v_{C1b} |_{t=t_2} = v_{C2a} \sin \omega t + ZI_A = V_o - V_{in} \sin \omega t + V_{stack} - ZI_B \quad (4.42)$$

The voltage on C_{2a} can therefore be obtained: -

$$v_{C2a} = \frac{V_{in} \sin \omega t - V_{stack} + V_o}{2} \quad (4.43)$$

Another condition is again based on the current of i_{in} . i_{in} is formed by i_{in}' and the train of current of i_{Lr} . Therefore, the average current of i_{Lr} appeared at i_{in}' is: -

$$\frac{I_A + I_B}{\pi} \frac{2T_o}{T_S} k = I_{in} \sin \omega t \quad (4.44)$$

Another condition is based on the energy conversion. The input and output energy is conserved and hence: -

$$I_{in} = \frac{2V_o I_o}{V_{in}} \quad (4.45)$$

The operation principle is also divided into 4 stages for analysis. The equations for the 4 states are given as follows: -

(i) State I [t_0-t_1]

$$v_{C1a} = V_{in} \sin \omega t - I_A Z \cos \omega_o t \quad (4.48)$$

$$i_{Lr} = I_A \sin \omega_o t \quad (4.49)$$

$$v_{C1j} = v_{C2j} - I_A Z \cos \omega_o t \quad (4.50)$$

where $j=a, b, \dots, n-1$;

(ii) State II [t_1-t_2]

$$v_{C1a} = V_{in} \sin \omega t + I_A Z \quad (4.51)$$

$$i_{Lr} = 0 \quad (4.52)$$

$$v_{C1j} = v_{C2j} + I_A Z \quad (4.53)$$

(iii) State III [t_2-t_3]

$$v_{C1j} = (v_{C2j} - V_{in} \sin \omega t) + I_B Z \cos \omega_o (t - t_2) \quad (4.54)$$

$$i_{Lr} = -I_B \sin \omega_o (t - t_2) \quad (4.55)$$

$$v_{C1n-1} = (V_o - V_{in} \sin \omega t) + I_B Z \cos \omega_o (t - t_2) \quad (4.56)$$

(iv) State IV [t_3-t_4]

$$v_{C1j} = (v_{C2j} - V_{in} \sin \omega t) - I_B Z \quad (4.54)$$

$$i_{Lr} = 0 \quad (4.55)$$

$$v_{C1n-1} = (V_o - V_{in} \sin \omega t) - I_B Z \quad (4.56)$$

Impedance and resonant frequency are given by: -

$$Z = \sqrt{\frac{L_r}{(n-1)C_1}} \quad (4.57)$$

$$\omega_0 = \sqrt{\frac{1}{(n-1)L_r C_1}} = \frac{2\pi}{T_o} \quad (4.58)$$

The voltage on v_{C2j} is

$$v_{C2j} = \frac{n-j-1}{n-1} V_{in} \sin \omega t - \frac{jV_o}{n-1} \quad (4.59)$$

where $j = a, b, \dots$. Because there are $n-2$ C_1 capacitors, therefore j is equivalent to count for $n-2$ alphabets. The amplitude of the resonant currents during the State I and State II are: -

$$I_A = \frac{1}{2} \left(\frac{I_{in} \sin \omega t \pi T_S}{2T_o k} - \frac{\frac{n}{n-1} V_{in} \sin \omega t - \frac{V_o}{n-1}}{Z} \right) \quad (4.60)$$

$$I_B = \frac{1}{2} \left(\frac{I_{in} \sin \omega t \pi T_S}{2T_o k} + \frac{\frac{n}{n-1} V_{in} \sin \omega t - \frac{V_o}{n-1}}{Z} \right) \quad (4.61)$$

4.5 Design Methods

4.5.1. Conditions of Zero-current Switching

To achieve the operation of zero-current switching, which is similar to the circuits as described in Chapter 2, i_L needs to resonate to zero in both state I and III for all stages and in all the switching cycle over the 50Hz period. Let d_1 and d_2 be the duty ratios of gate signals of the transistors, S_1 and S_2 , respectively, and assuming the circuits are lossless, conditions of obtaining zero-current switching of all circuits in the family are: -

$$d_1 T_s > \frac{\pi}{\omega_0} \quad (4.62)$$

and

$$d_2 T_s > \frac{\pi}{\omega_0} \quad (4.63)$$

4.5.2 Selection of Resonant Components

The resonant components can therefore be calculated by angular frequency and impedance from the following equations: -

$$\omega_0 = \frac{1}{\sqrt{(n-1)L_r C_1}} \quad (4.64)$$

$$Z = \sqrt{\frac{L_r}{(n-1)C_1}} \quad (4.65)$$

The resonant capacitor C_1 and inductor L_r as given as follows: -

$$C_1 = \frac{1}{2Z\omega_0} = 0.22\mu F$$

$$L_r = \frac{Z}{\omega_0} = 1\mu H$$

4.5.3 Rating of Components

The voltage rating of S_1 and S_2 is V_{in} . The voltages rating of all diodes are also equal to V_{in} . The voltage rating for C_{2j} is varied with j and can be calculated by the following equation: -

$$v_{C2j} = \frac{n-j-1}{n-1}V_{in} + \frac{jV_o}{n-1} < V_{in} + V_o \quad (4.66)$$

The voltage rating for C_1 is: -

$$v_{C1a} = V_{in} + I_A Z \quad (4.67)$$

$$v_{C1j} = \frac{n-j-1}{n-1}V_{in} + \frac{jV_o}{n-1} + I_A Z \quad (4.68)$$

4.6 Discussion

The circuit waveforms of the AC-DC converters using quasi-resonant switched-capacitor techniques have been analyzed. It has been found that C_2 is not a “pure” DC as in the case of the DC-DC conversion and it consists of the low frequency, ω , and the voltage, V_o . However, for C_1 case, C_{1a} is the combination of low frequency ω and ω_o . For C_{1b} , C_{1c} ,..., there is also a fraction V_o with the AC components appeared on their voltages.

The amplitude of the resonant current is expressed as I_A and I_B in the State I and II respectively. I_B is usually larger than I_A . They are the functions of resonant frequency, switching frequency, output voltage and VCO variable k . The resonant current is regulated by k to control the shape of the input current.

4.7 Summary

This chapter describes the operation of the step-up circuit and its application in the AC-DC power conversion. The analysis of the circuit is different from the DC-DC counterpart because the driving signal varies with the frequency of the input voltage (i.e.50Hz). The zero-current switching can be attained with the use of the switching components, transistors and diodes and the current waveforms provided from the components are all sinusoidal. Properly controlling the transistor S_1 and S_2 , all the currents resonates from zero and finish at zero values. Therefore zero-current switching can be attained. The circuit is also so-called continuous mode because the input current is formed by trains of continuous resonant inductor current. In each switching period, the resonant current raises from zero and finishes at zero. The frequency of appearing of the switching period is to control the shape of the input current which is realised by VCO.

Chapter 5 Control of Power Factor Correction Zero-current Switching Switched-capacitor AC-DC Converters

5.1 Introduction

The concept of proposed PFC controller applying in zero-current switching quasi-resonant switched-capacitor converter has been introduced in Chapter 3. The practical PFC controller circuit diagram will be developed and analysed in this chapter.

5.2 Controller Design

The gate drive and the controller for the AC-DC PFC circuit are shown in Fig 4.1. Table 5.1 shows the specification.

Table 5.1 Design specification of Controller

Controller IC	CD4046
Signal Inverting IC	CD4093
Controller Supply Voltage	15V
Output Frequency	100 kHz - 200 kHz
Reference Sine-wave Voltage	0V – 25V (50Hz)

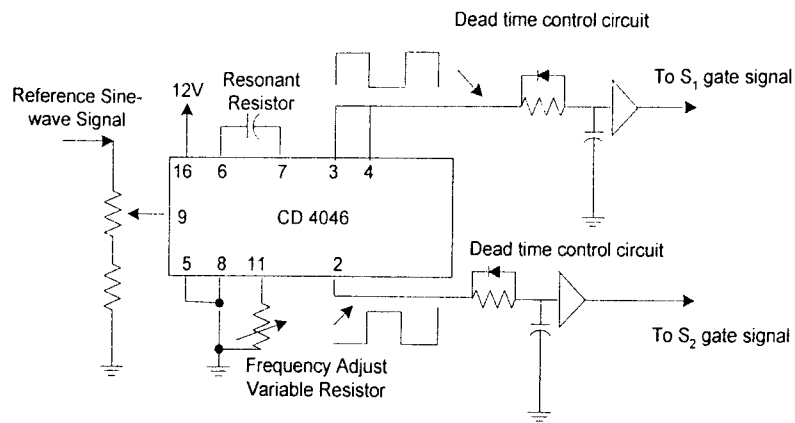


Fig. 5.1 Circuit diagram of power factor correction controller for zero-current switching switched-capacitor quasi-resonant AC-DC converter

5.3 Simulation Analysis

The circuit simulation package, Saber, has been used to simulate the PFC controller applying in the zero-current switching switched-capacitor quasi-resonant AC-DC converter. The simulation results are given as follows: -

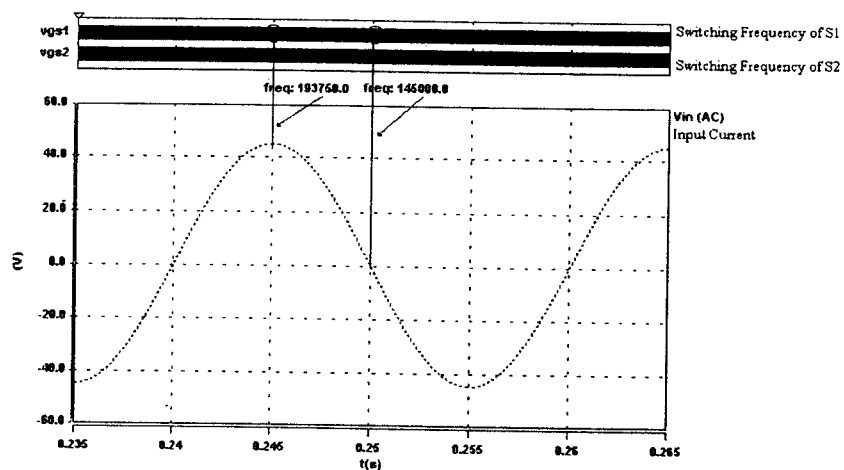


Fig. 5.2 Relationship between the main input voltage and PFC controller gate signal frequency

The transistor gate signal output including the duty ratio and frequency is programmed according to the voltage amplitude as discussed in chapter 3. Fig. 5.2 has shown the relationship between the main input voltage amplitude and the PFC controller gate signal frequency. In this simulation, the relationship between the main input voltage amplitude and the PFC controller gate signal frequency was analyzed for detailed demonstration (Fig. 5.3 – 5.5).

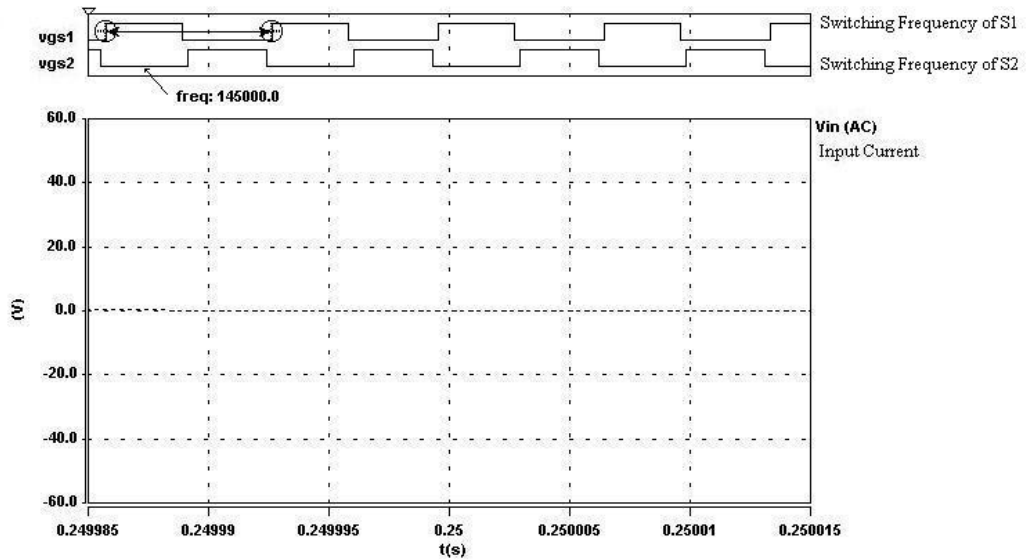


Fig. 5.3 PFC controller gate signal frequency at main input voltage equal to 0V

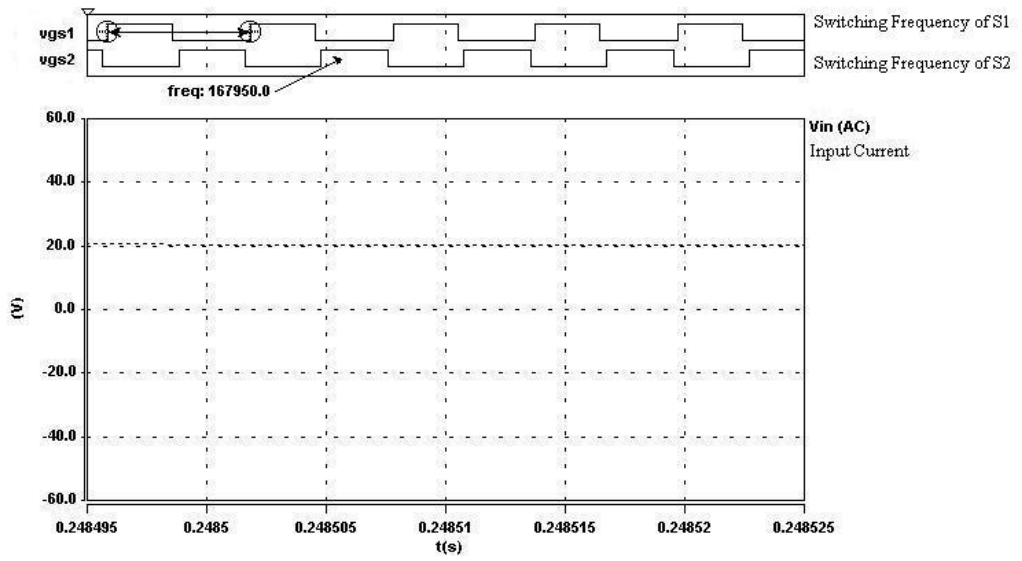


Fig. 5.4 PFC controller gate signal frequency at main input voltage equal to 20V

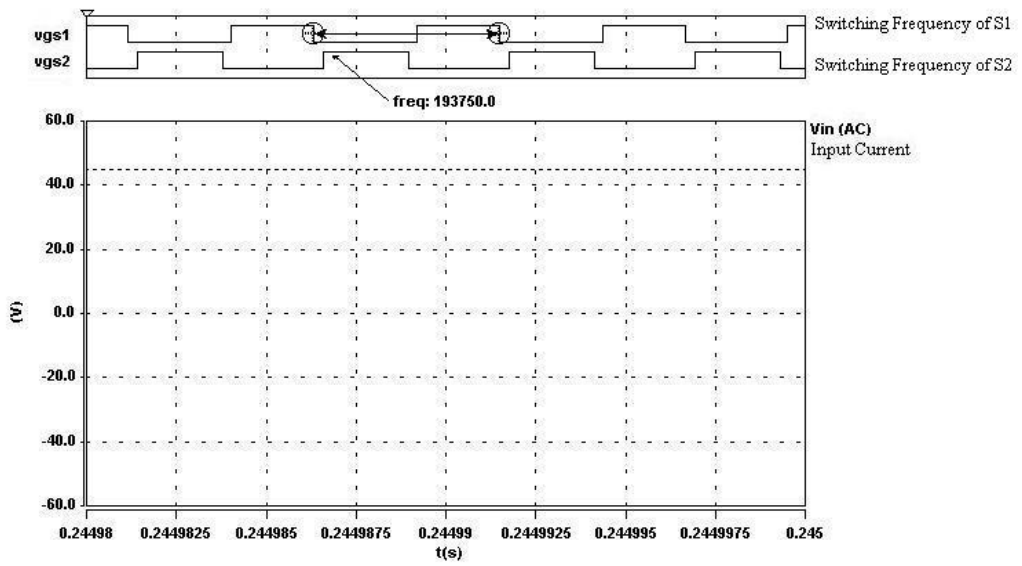


Fig. 5.5 PFC controller gate signal frequency at main input voltage equal to 40V

The relationship between the main input voltage amplitude from 0 to 40V and resonant inductor current i_{Lr} was shown in Fig. 5.6 – 5.10.

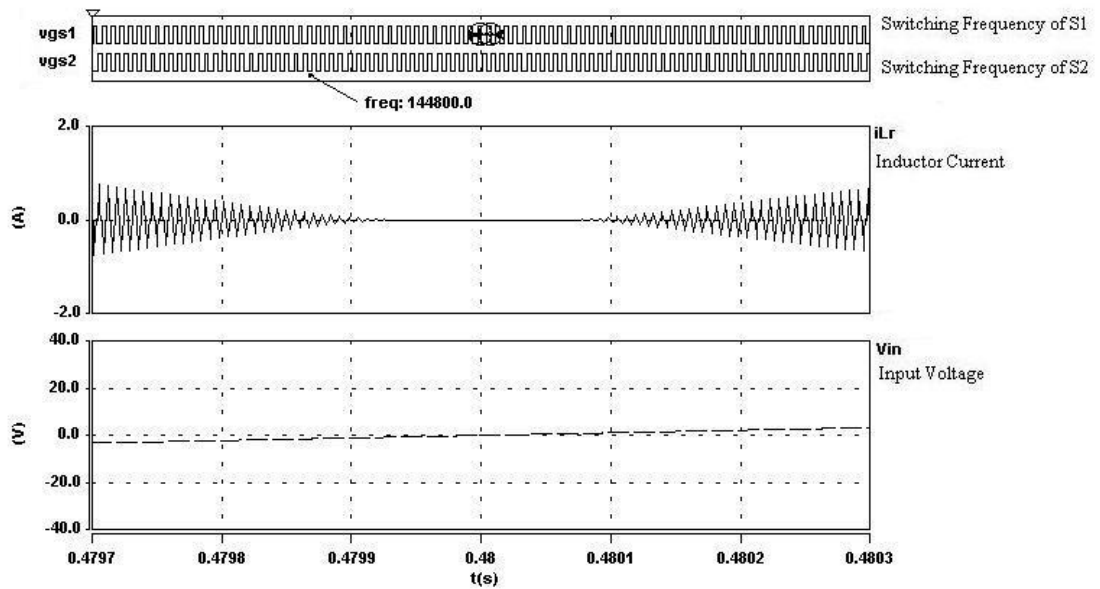


Fig. 5.6 Resonant current at main input voltage equal to 0V

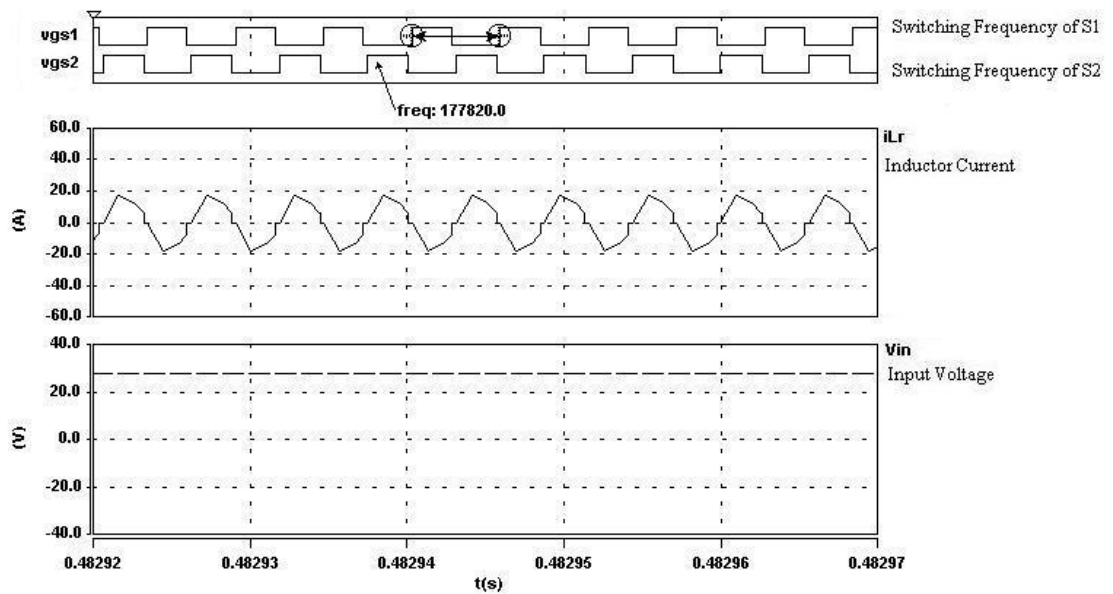


Fig. 5.7 Resonant current at main input voltage equal to 30V

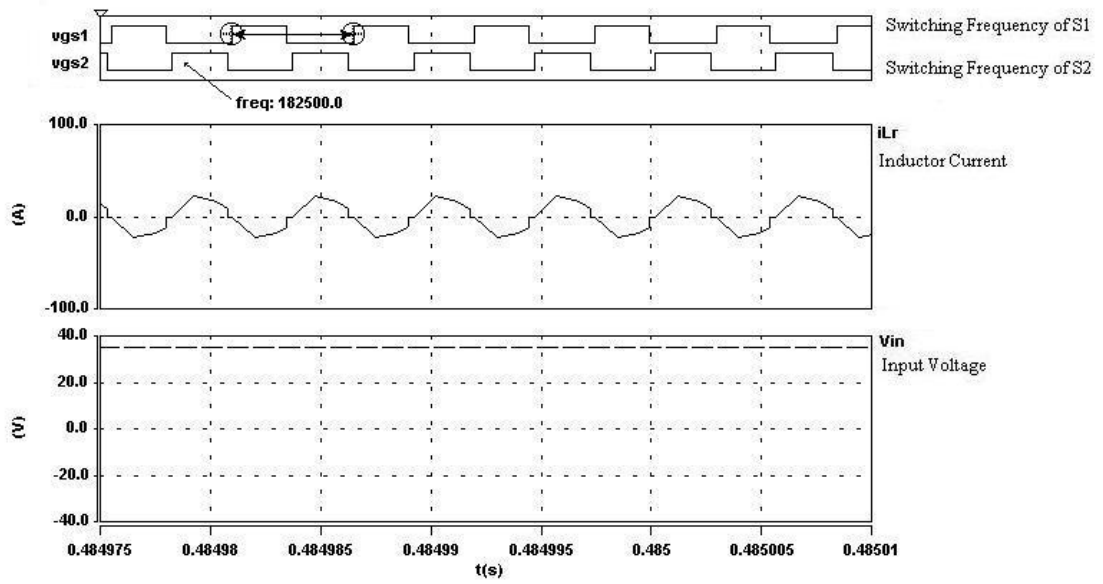


Fig. 5.8 Resonant current at main input voltage equal to 40V

Fig. 5.9 shows the conduction relationship between the resonant inductor current i_{Lr} , switching frequency of PFC controller, main input voltage amplitude and output voltage. The simulation results show that the resonant inductor current i_{Lr} conducts continuously at difference main input voltage amplitude. Fig 5.10(a) - 5.10(d) shows the simulation results of the converters. It is observed that the waveforms pattern is consistent with the theoretical prediction. ZCS can be achieved. It confirms that the proposed theory is followed.

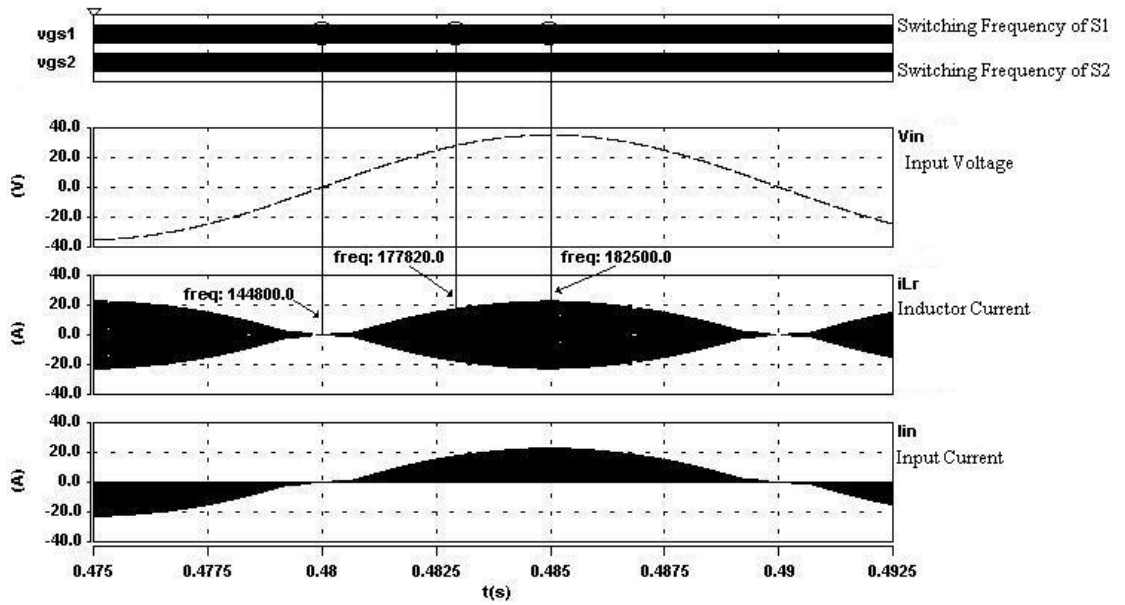


Fig. 5.9 Relationship of resonant current, main input voltage and switching frequency of PFC controller

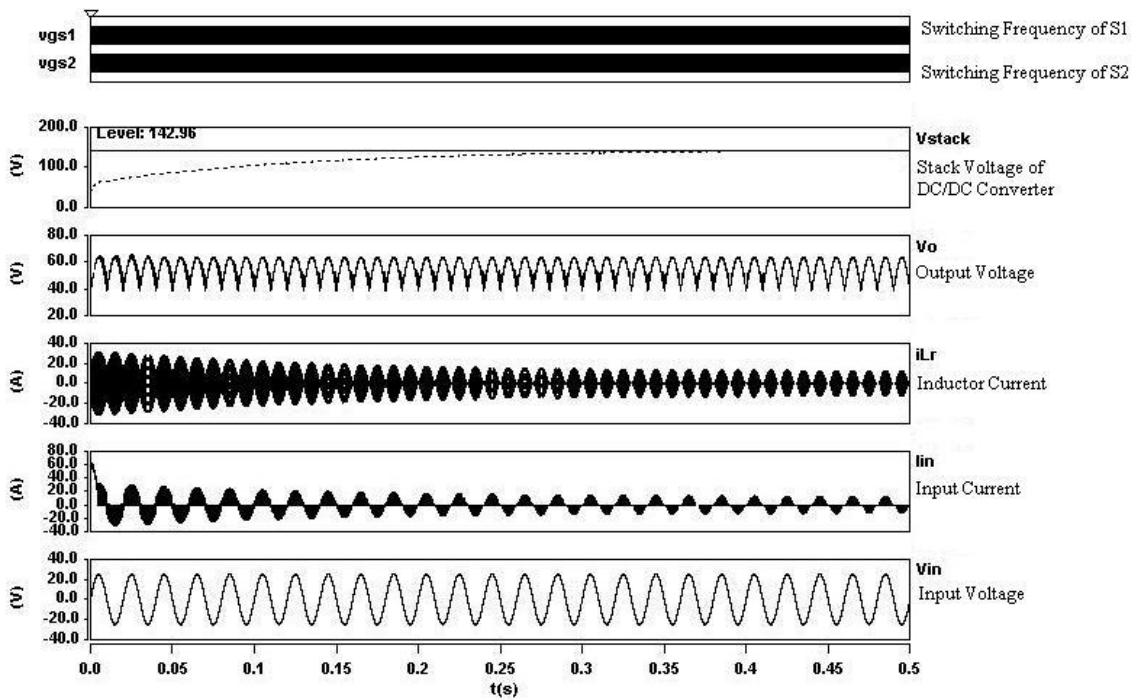


Fig. 5.10(a) Outline of the simulation result for Triple-mode PFC ZCS quasi-resonant switched-capacitor AC-DC converter

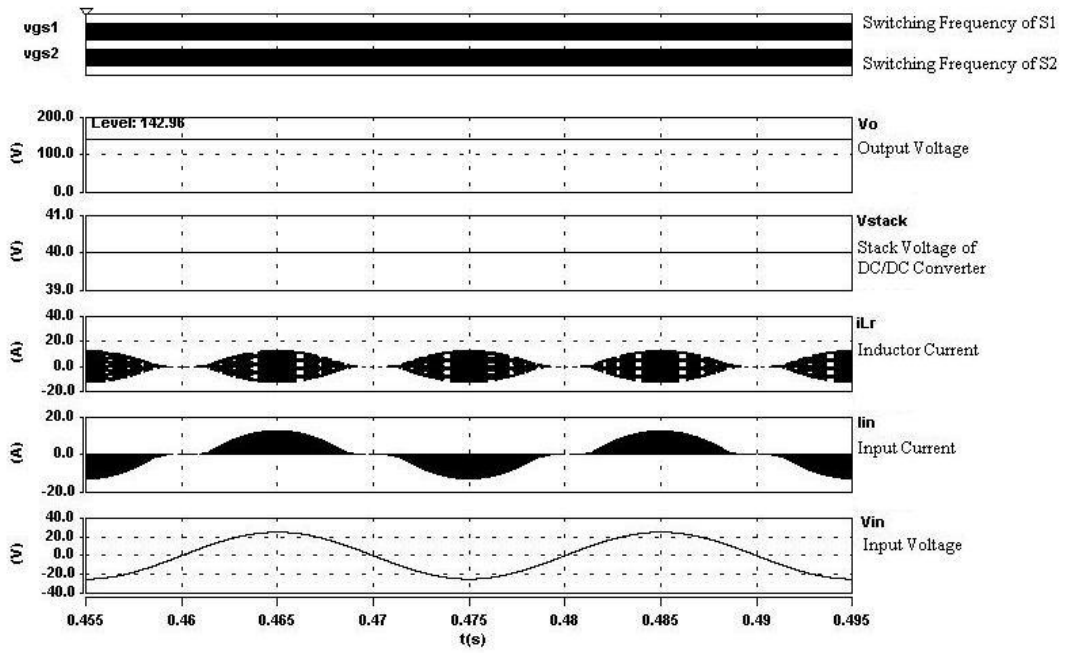


Fig. 5.10(b) Outline of the simulation result for Triple-mode PFC ZCS quasi-resonant switched-capacitor AC-DC converter

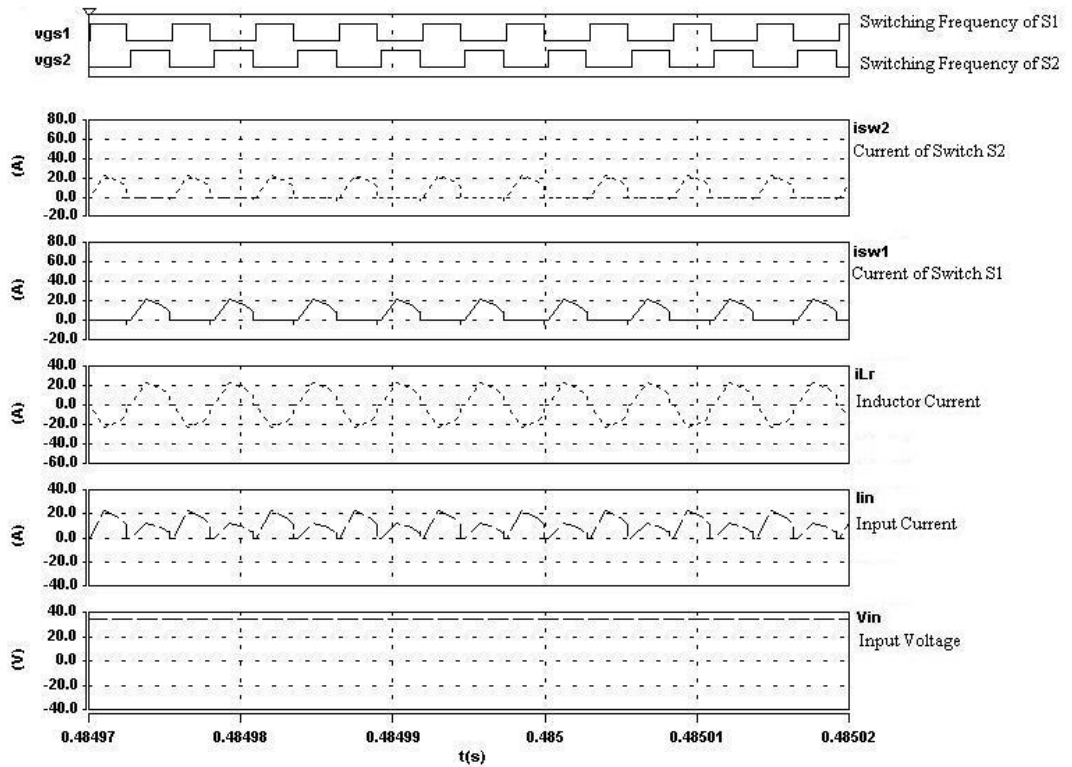


Fig. 5.10(c) Outline of the simulation result for Triple-mode PFC ZCS quasi-resonant switched-capacitor AC-DC converter

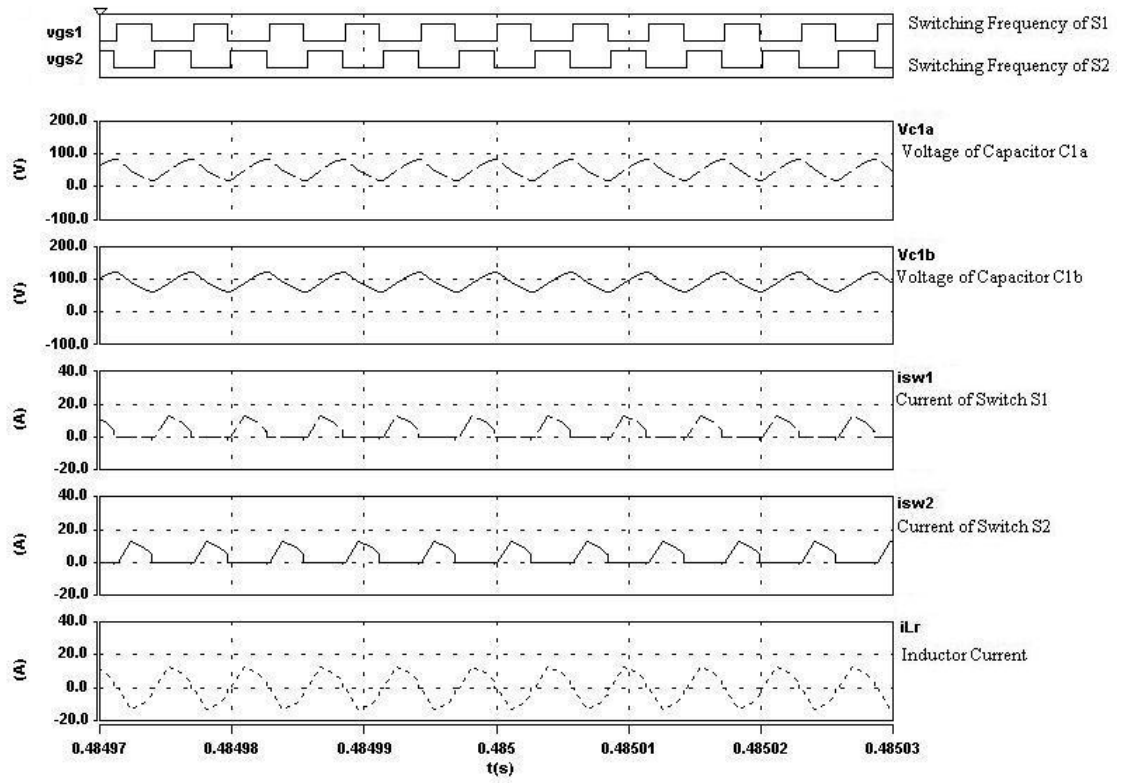


Fig. 5.10(d) Outline of the simulation result for Triple-mode PFC ZCS quasi-resonant switched-capacitor AC-DC converter

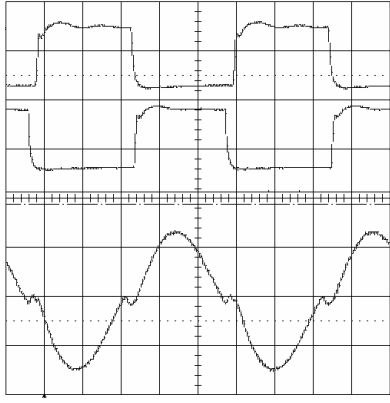
Table 5.2 Specification and component values of prototype power factor correction zero-current switching switched-capacitor triple-mode quasi-resonant AC-DC converters

Input voltage	AC 25V(RMS)
Output voltage	75V
Output power	10W - 100W
Switching frequency	100 – 200 kHz
Q ₁ and Q ₂	IRF630
D ₁ and D ₂	MBR10100
C _{1a} and C _{1b}	0.22 μ F
C _{2a} and C _{2b}	100 μ F
L _r	1 μ H

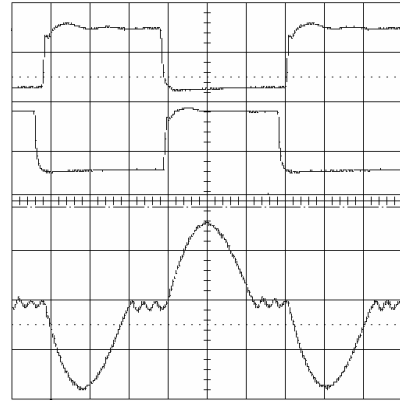
5.4.2 Operation Under DC condition

The PFC controller generates the variable frequency to control the switching devices. The circuit is firstly examined under DC input condition to examine the circuit components. Fig. 5.12 has indicates the resonant inductor current in different switching frequencies under fixed supply voltage.

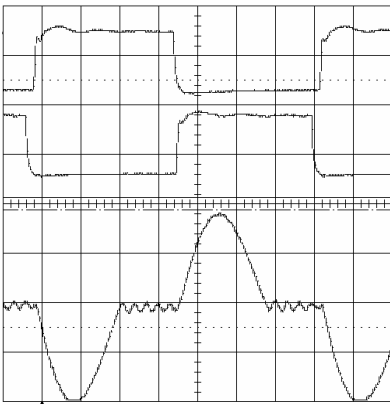
It is observed that the switching capacitor resonant tank is found to perform zero-current switching when the excitation frequency is varied up to 200 kHz. This confirms the variable frequency operation for the system.



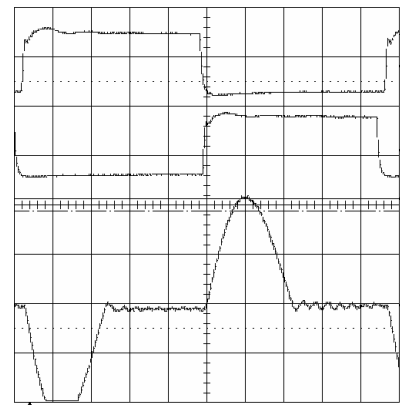
(a) 200 kHz, Time base = $1\mu\text{s}/\text{div}$



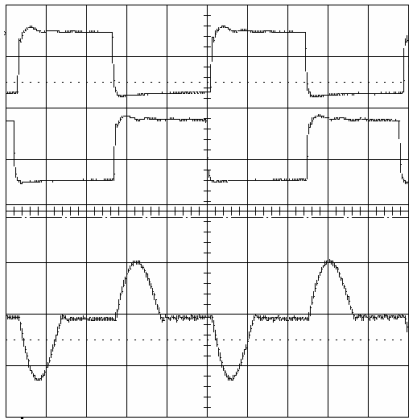
(b) 160 kHz, Time base = $1\mu\text{s}/\text{div}$



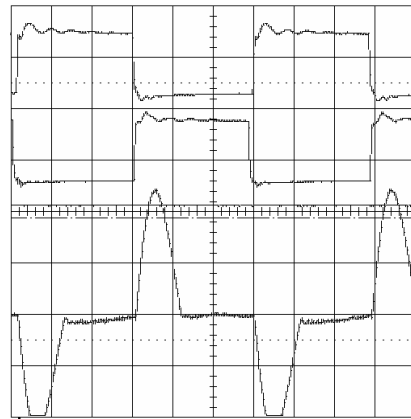
(c) 140 kHz, Time base = $1\mu\text{s}/\text{div}$



(d) 110 kHz, Time base = $1\mu\text{s}/\text{div}$



(e) 100 kHz, Time base = $2\mu\text{s}/\text{div}$



(f) 83 kHz, Time base = $2\mu\text{s}/\text{div}$

Upper trace: Gate signal of S_1 , 20V/div, Middle trace: Gate signal of S_2 , 40V/div,

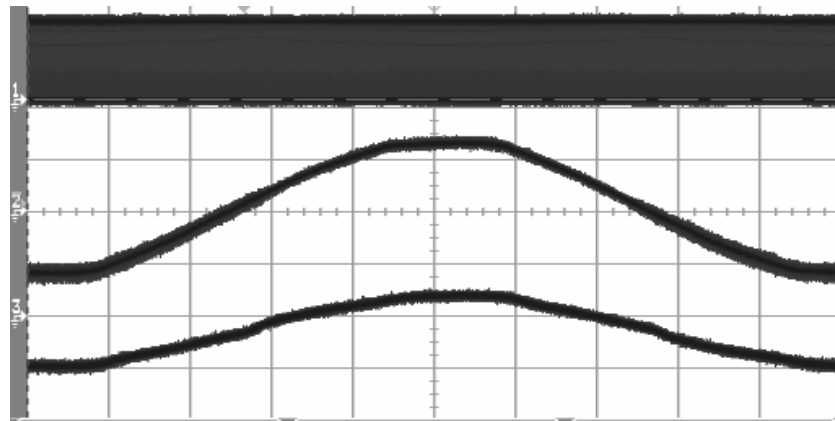
Lower trace: L_r current, 5A/div

Fig. 5.12 Measured result of resonant inductor current at difference switching

frequency

5.4.3 Initial Examination of VCO

The frequency variation with respect to the input voltage amplitude is illustrated in Fig 5.13. It is clear that the switching frequency of the gate signals varies from very low (near the zero-crossing) to high value (near the peak or trough).



Upper trace: Gate signal of S_1 , 20V/div,

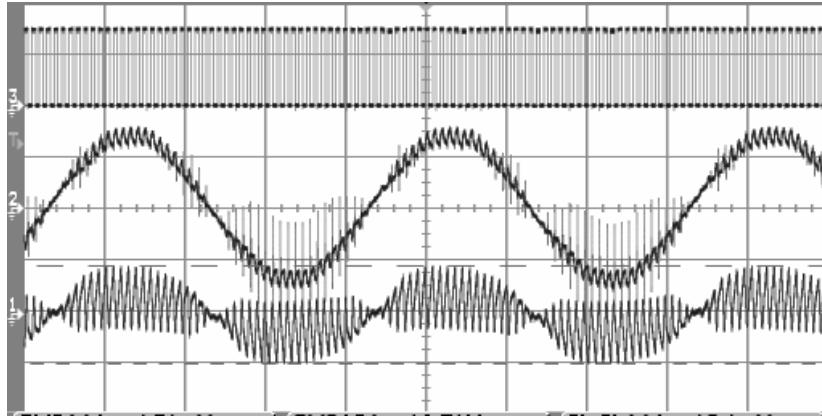
Middle trace: Input Voltage of V_{in} , 40V/div,

Lower trace: Input current of i_{in} , 5A/div

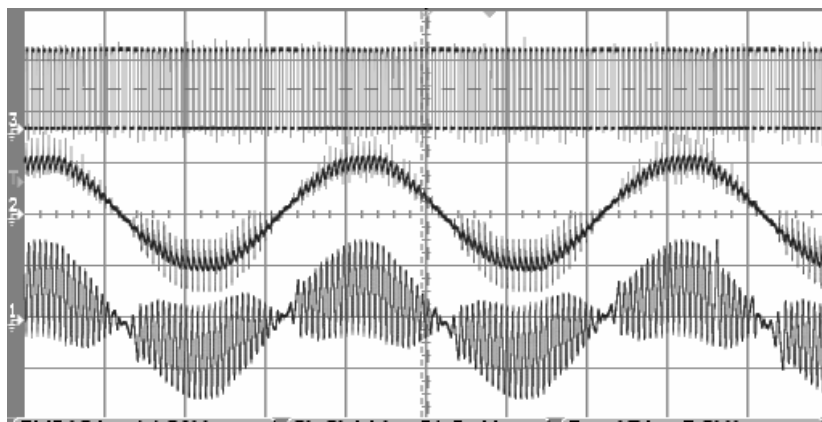
Fig. 5.13 Measured relationships between the main input voltage and PFC controller gate signal frequency

5.4.4 Examination of the AC-DC converters under various operation

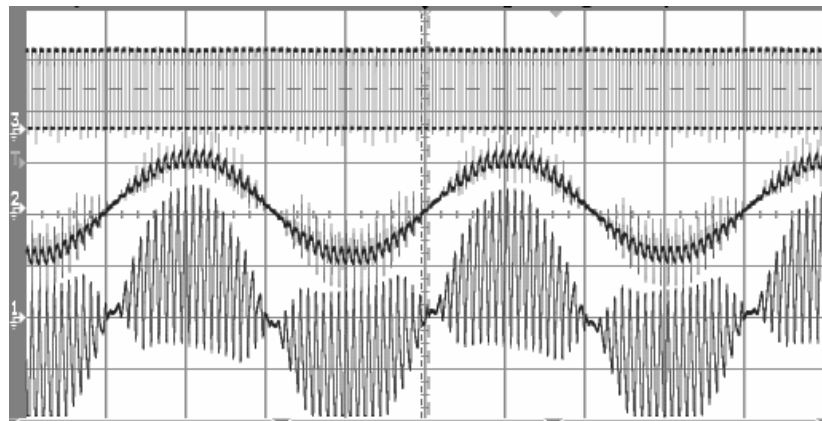
Fig 5.14 and Fig 5.15 shows the experimental waveforms of the AC-DC converter. It can be seen that the input current is a continuous with a sinusoidal waveforms. The waveforms are needed to filter by a low pass filter and DC/DC converter circuit in order to eliminate the low order frequencies and shaping the input current.



(a) Non-filtering, 50W power output



(b) Non-filtering, 70W power output

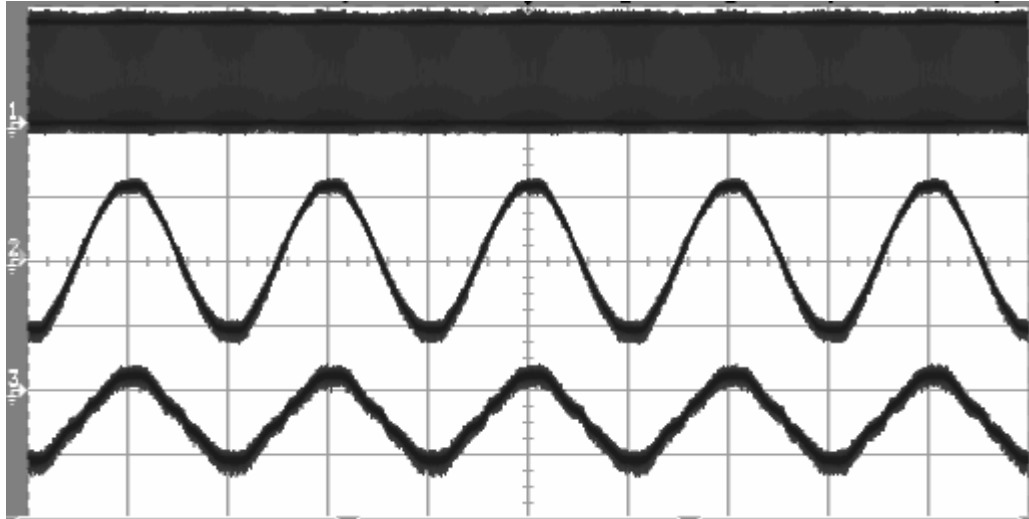


(c) Non-filtering, 90W power output

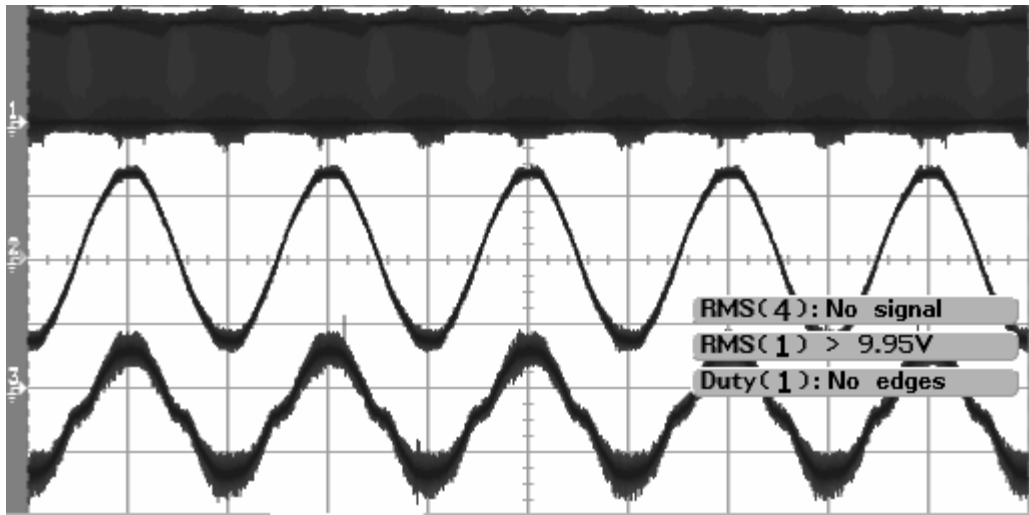
Upper trace: Gate signal of S_1 , 20V/div, Middle trace: Input Voltage of V_{in} , 40V/div,

Lower trace: Input current of i_{in} , 5A/div

Fig. 5.14 Measured Non-filtering input voltage and current of triple-mode PFC zero-current switching quasi-resonant switched-capacitor AC-DC converter



(a) Filtering, 70W power output



(b) Filtering, 100W power output

Upper trace: Gate signal of S_1 , 20V/div,

Middle trace: Input Voltage of V_{in} , 40V/div,

Lower trace: Input current of i_{in} , 5A/div

Fig. 5.15 Measured Filtering input voltage and current of triple-mode PFC zero-current switching quasi-resonant switched-capacitor AC-DC converter

After applying the filtering circuit the power factor of the converter is over 0.9 at wide range of output power as shown in Fig. 5.18 and the efficiency and voltage

conversion ratio has been measured as shown in Fig. 5.16 and 5.17. Greater than 90% efficiency can be obtained for power handling from 20W to 90W. The switching frequency of the VCO is programmed to vary from 100 kHz to 200 kHz. The conversion ratio of the converter is shown in Fig 5.16. It indicates that the regulation of the converter is not very good because the VCO has not been optimised. The measured efficiency of the converter is shown in Fig 5.17. The efficiency is quite good and achieves over 90% for higher power.

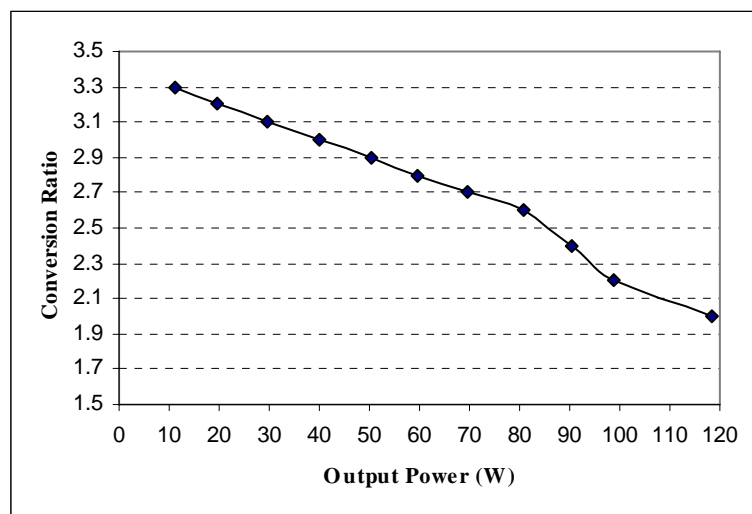


Fig. 5.16 Measured voltage conversion Ratio and output power of triple-mode PFC zero-current switching quasi-resonant switched-capacitor AC-DC converter

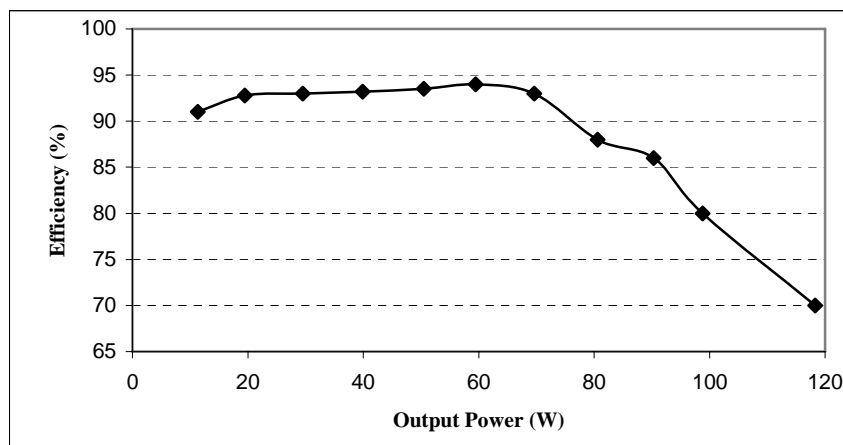


Fig. 5.17 Measured efficiency and output power of triple-mode PFC zero-current switching quasi-resonant switched-capacitor AC-DC converter

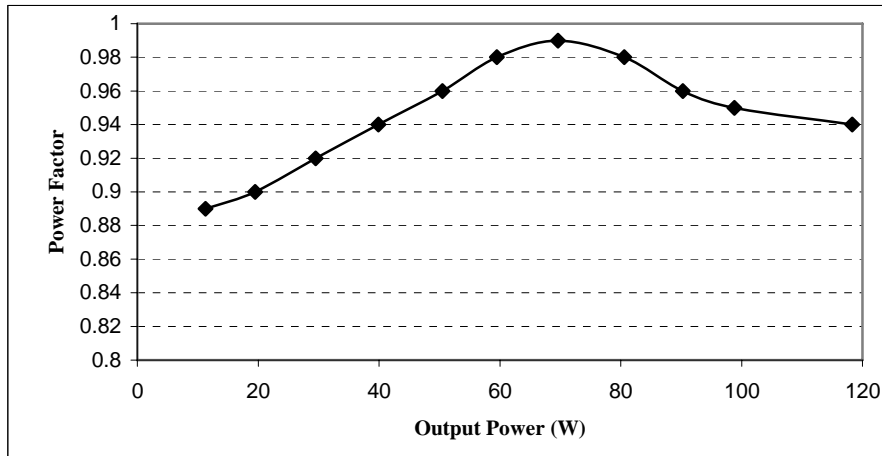


Fig. 5.18 Measured power factor and output power of triple-mode PFC zero-current switching quasi-resonant switched-capacitor AC-DC converter

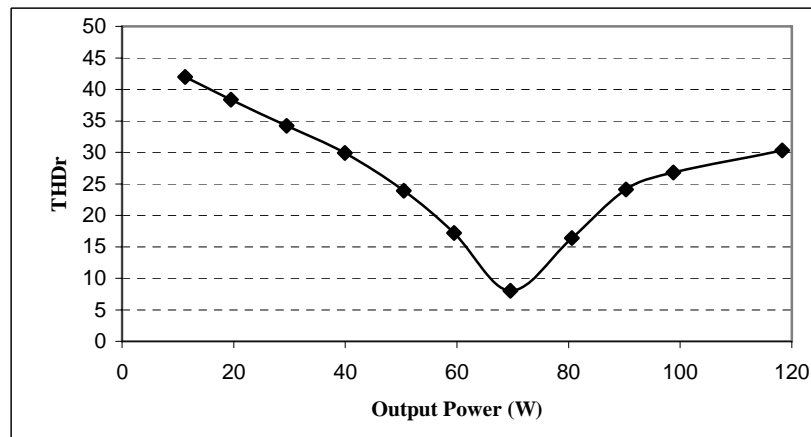


Fig. 5.19 Measured THD and output power of triple-mode PFC zero-current switching quasi-resonant switched-capacitor AC-DC converter

Finally, the input current should be fulfilled by a low-pass filter in order to remove the high frequency components. Fig 5.15(a) and 5.15(b) shows the filtered input currents. A sinusoidal input current is observed. The measurable current is very quite sinusoidal with some distortion near the zero-crossing. This is a common feature for single phase AC-DC power converters. However, the result shows a high portion of distortion and can be further improved by proper tuning of the VCO, low pass filter design and DC/DC shaping circuit.

The high efficiency is mainly obtained by the quasi-resonant zero-current switching. This type of converter, same as the zero-current switching quasi-resonant DC-DC converters, can control the charge and discharge of the switched-capacitor in each half resonant period. Using variable switching frequency and DC/DC convert shaping circuit, the current waveform at the input side can be shaped appropriately. The result has been shown in Fig.5.12. The zero-current switching technique applying in the converter can reduce the switching loss of switching devices. But the drain-to-source junction capacitors of the transistors introduce switching losses and are directly proportional to the switching frequency. However, higher fraction and higher multiplication conversion ratio [4.2, 5.1] of the converter require more diodes for routing the charging and discharging of the capacitors current. As the result, the efficiency of the converters will be lower. This problem is mainly due to the forward voltage of the diodes. So, the schottky diodes were used in this converter to reduce the higher conduction loss and diode forward voltage.

Fig. 5.9(a) and 5.9(b) will shown the conduction relationship between the resonant inductor current i_{Lr} , switching frequency of PFC controller, main input voltage amplitude and output voltage value. The simulation result shown the resonant inductor current i_{Lr} conducted at continuously at difference switching frequency by adding the DC/DC converter shaping circuit otherwise, the input current stops flowing to the bridge rectifier and converter was caused by the reverse bias of the diodes. Thus, the input current shape of the measurable result is continuous form shown in Fig. 5.15. The input voltage and current of the converter has been programmed to be in phase and hence high power factor as

shown in Fig. 5.15. The input current is found to be nearly sinusoid wave after LC filter circuit has been added between the main input supply and bridge rectifier for removal of the switching pulses. It is confirmed that the proposed PFC controller can provide easy way for PFC in zero-current switching quasi-resonant switched-capacitor converters. The measured 0.99 power factor and the measured total harmonic distortion after the filtering is 8 % at 70W output power. This is a promising figure for a simple approach of PFC.

5.5 Summary

In this chapter, a voltage control frequency technique using in PFC controller for triple-mode zero-current switching quasi-resonant switched-capacitor converter has been examined based on 110W output power experimental results. Mathematical modeling, generalized equation, computer simulation and experiments have been presented. There is only a very simple PFC controller using voltage-control- frequency technique applying in the zero-current switching quasi-resonant switched-capacitor converter circuit. Thus, no complicated circuit topology is required in this PFC controller. No current mode sensing is needed and the controller is basically operates under open current loop with continuous inductor current manner. All switching devices in these circuits are under zero-current switching condition. Both switching loss and EMI have been reduced. High efficiency can then be obtained. From the experiment, it shows that the efficiency of the PFC converter can be around 90%. Also, the power factor is improved significantly as compared to simple capacitive type bridge rectifier.

Chapter 6 Conclusions and Recommendations

6.1 Conclusions

The contributions have been concluded in the study as follows: -

- (i) The step-up zero-current switching quasi-resonant switched-capacitor DC-DC converters have been proposed. The converters produce different step-up voltage conversion ratios and all switching devices of the converters are under the zero-current switching condition to reduce the current stress of the transistors and to provide high power applications other than the conventional switched-capacitor converters.
- (ii) Mathematical analysis provides equations for triple-mode zero-current switching quasi-resonant switched-capacitor DC-DC converters circuits systematically. The step-down inverting circuit and step-up triple-mode zero-current switching quasi-resonant switched-capacitor DC-DC converters are also simulated by computer and tested in laboratory to verify the switching devices that are under zero-current switching and obtain high efficiency characteristics of the converters.
- (iii) A power factor correction controller design concept and operation principle has been developed. The variable switching frequency control technique for zero-current switching quasi-resonant switched-capacitor AC-DC converters has been proposed. The controller switching frequency is

depending on the reference input voltage amplitude. According to this concept, the designed PFC controller can achieve high power factor. Besides, input voltage and current are in phase with sinusoid shape.

- (iv) The proposed circuit of PFC controller for step-up, step-down and inverting mode zero-current switching quasi-resonant switched-capacitor converter has been introduced. The practical PFC controller circuit diagram has been developed and analysed. Mathematical analysis provides generalized equations for n-mode PFC controlled step-up circuits systematically. The step-up triple-mode PFC circuit of zero-current switching quasi-resonant switched-capacitor AC-DC converters have been simulated by Saber circuit simulator and tested in laboratory to verify the zero-current switching, high efficiency and power factor of the converters.
- (v) The simulation result shown the resonant inductor current i_{Lr} conducted at continuously at different switching frequencies by adding the DC/DC converter shaping circuit otherwise, the input current stops flowing to the bridge rectifier and converter was caused by the reverse bias of the diodes. Thus, at the design state, the DC/DC converter converted the stack-up voltage connected to the ac power source in order to shaping the input ac current nearly sinusoidal. Finally, the low pass filter also applied to filtering the input of the converter. The experiment has verified that the relationship between the amplitude of resonant inductor current i_{Lr} and switching frequency of PFC controller, main input voltage amplitude and output voltage value.

- (vi) A proposed PFC triple-mode step-up zero-current switching quasi-resonant switched-capacitor AC-DC converter has been analysed and examined. The experimental results have confirmed that the voltage-controlled-frequency technique applying in PFC control can obtain high power factor and efficiency.

6.2 Recommendations for Further Researches

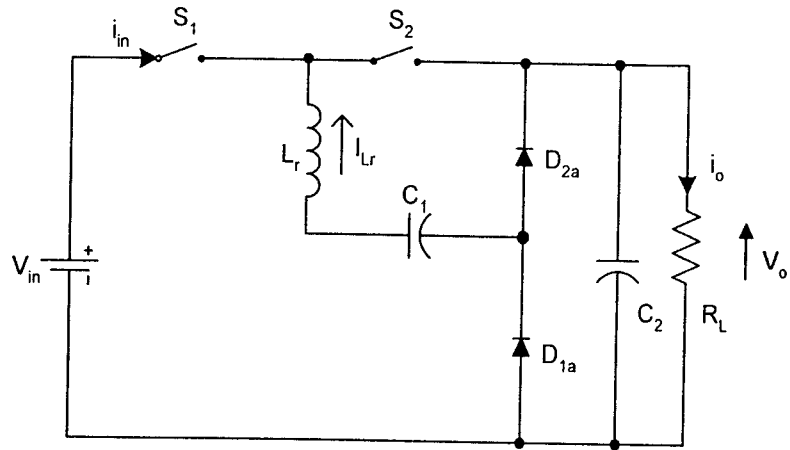
Regarding the PFC triple-mode step-up zero-current switching quasi-resonant switched-capacitor AC-DC converter, areas of further study are recommended as follows: -

- (i) Develop a zero-voltage switching circuit to reduce the switching loss and obtain the soft-switching.
- (ii) Develop a PWM controller for power factor correction applying in zero-current switching quasi-resonant switched-capacitor AC-DC converter.
- (iii) Develop a more precise model, such as non-linear modeling for power factor correction controller for computer simulations.
- (iv) Investigate the range of the switching frequency in different reference input voltages related to the voltage conversion.

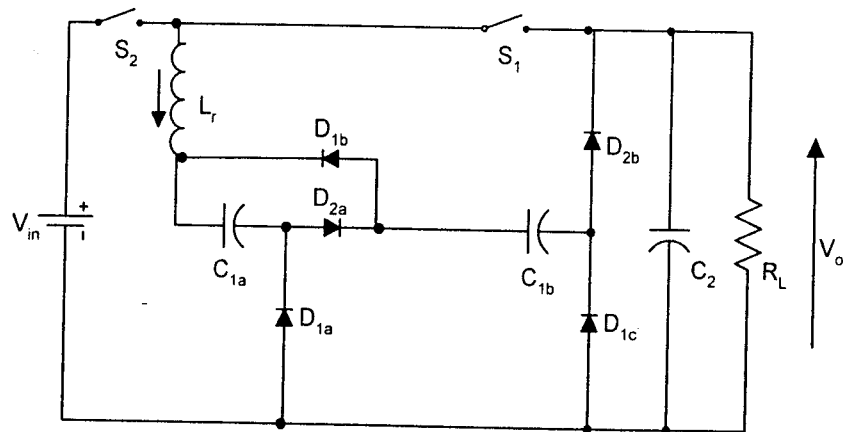
- (v) Perform higher power level testing for step-up zero-current switching quasi-resonant switched-capacitor AC-DC converter. To analyze the efficiency in high power application with respect to power loss of each component.
- (vi) Perform higher voltage input level testing for step-up zero-current switching quasi-resonant switched-capacitor AC-DC converter.
- (vii) Study the resonant current conduction period related to the switching frequency in high power output.
- (viii) Study the PWM control applying in the voltage-controlled-frequency technique for PFC zero-current switching quasi-resonant switched-capacitor AC-DC converter.
- (ix) Study the THD method applying for PFC controller to reduce the harmonics of the converter.

Appendix A

Family of zero-current switching quasi-resonant step-down switched-capacitor converters

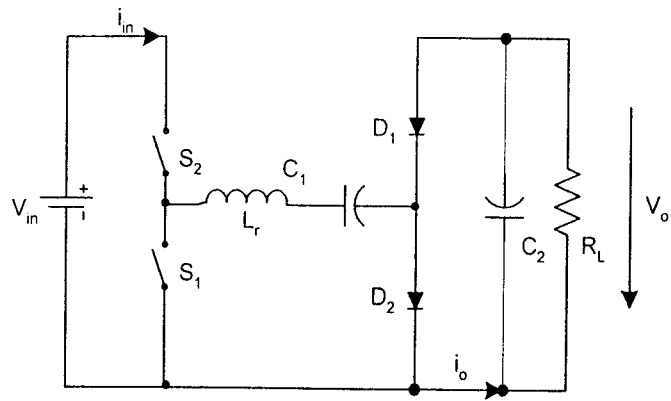


(a) 1/2-mode

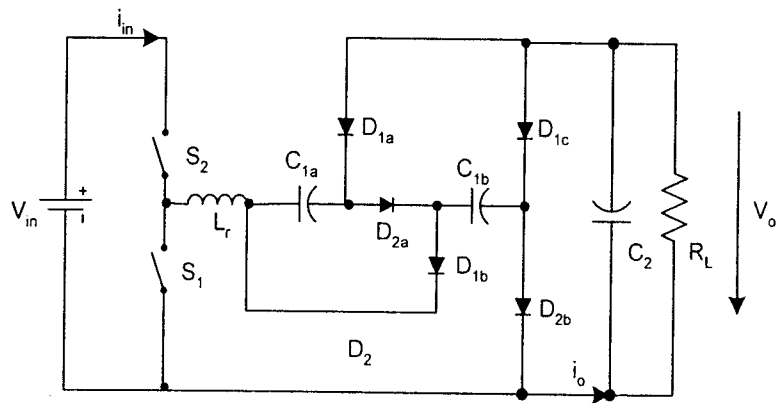


(b) 1/3-mode

Fig. A1 Circuit diagrams of zero-current switching quasi-resonant step-down converters



(a) Inverting mode



(b) Inverting 1/2-mode

Fig. A2 Circuit diagrams of zero-current switching quasi-resonant inverting mode converters

A simple switched-capacitor cell for step-up mode is proposed as shown in Fig. A3. This switched-capacitor cell consists of only one capacitor and two diodes. By adding the switched-capacitor cell to the converters, voltage conversion ratios of the converters increase. No additional switching device is

required for changing the voltage conversion ratio. This means that switching devices and drive circuits for additional switched-capacitor cell can be fixed. Hence the manufacturing cost and transistor drive loss decrease.

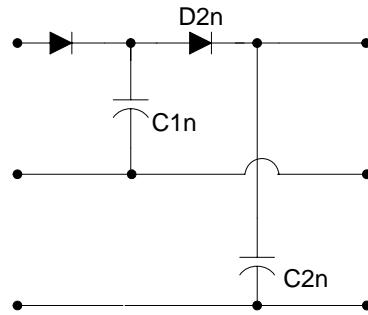
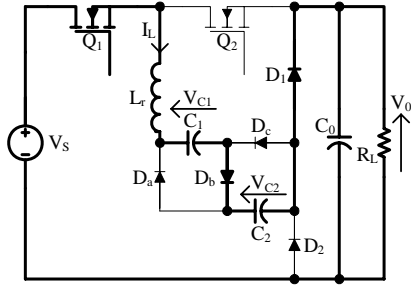


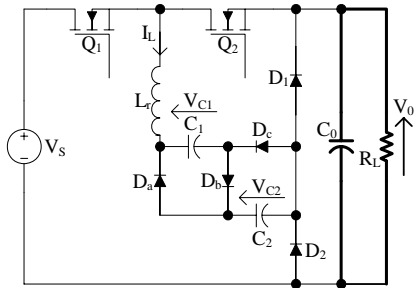
Fig. A3 Switched-capacitor cell for step-up mode

Principles of Operation

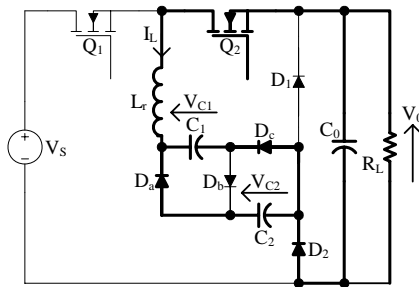
Four operation states of the proposed inverting 1/2-mode step-down zero-current switching quasi-resonant switched-capacitor DC-DC converter shown in Fig. A4 and the equivalent circuits of each state of operation of the inverting 1/2-mode switched-capacitor resonant step-down DC-DC converter.



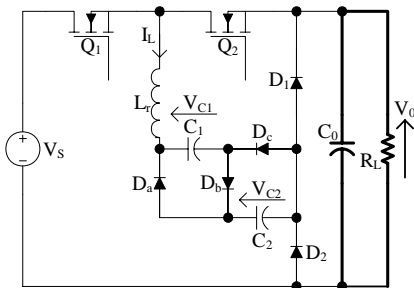
(a) State I



(b) State II



(c) State III



(d) State IV

Fig. A4 States of operation of inverting -1/2-mode switched-capacitor resonant step-down converter

(i) *State I* [$t_0 - t_1$]

At the time state t_0 , Q_1 is switched on while Q_2 is switched off. The charging current from the source passes through the components D_b , D_1 , L_r and charging the C_1 and C_2 in series. At the same time, output capacitor C_0 is discharged to the load. Zero-current switching-on of Q_1 is achieved by the inductor current i_L resonating with C_1 and C_2 in a sinusoidal manner. Hence, the resonant inductor current decreases from zero at t_0 , to the negative peak, and then increases from the peak to zero. As the result, it reaches zero again at t_1 . The inductor current i_L reaches zero and the input current are equal to zero. Then, the diodes D_b and D_1 stop the resonance at time t_1 . At this time, C_0 is discharged to the load resistor R_L .

(ii) *State II* [$t_1 - t_2$]

In this state Q_1 keep on and Q_2 is still off. At time t_1 , the inductor current i_L reaches zero. The resonance stops by the reverse bias of the diodes. At this time, the current maintains at zero and the output capacitor C_0 is discharged to the load resistor R_L .

(iii) *State III* [$t_2 - t_3$]

After State II, the switch Q_1 is switched off and Q_2 is switched on at time t_2 . The inductor current i_L is zero at time instant t_2 when Q_1 is switched off. At the time t_2 , the Q_2 is zero-current switched on while Q_1 is zero-current switched off. At the same time, C_1 and C_2 are discharged to the load through L_r , D_a , D_b and D_2 .

This is most similar to State I, the resonant current starts at time instant t_2 in a sinusoidal manner and hence, Q_2 is switched on under zero-current switching condition. The inductor current i_L starts decreasing from zero at t_2 to the peak and then increases to zero at t_3 .

(iv) State IV [$t_3 - t_4$]

This state is similar to state II. The switch Q_1 is off and Q_2 is on. The resonance inductor current i_L is stopped by the reverse bias of the diodes. So, the inductor current is zero in this operation state and the output capacitor C_0 start discharging to the load as the same time. That means the switching component Q_2 is switched off under zero-current at t_4 .

Mathematical Analysis

(i) The equations of State I [$t_0 - t_1$] are: -

$$V_s = L_r \frac{di_L}{dt} + 2v_c \quad (A1)$$

$$i_L = C \frac{dv_c}{dt} \quad (A2)$$

By solving the differential equations (2.1) and (2.2),

$$v_c = \frac{V_s}{2} - \frac{V_s - 2V_{c0}}{2} \cos \omega_0 (t - t_0) \quad (A3)$$

$$i_L = \frac{V_s - 2V_{c0}}{Z_0} \sin \omega_0 (t - t_0) \quad (A4)$$

where V_{C2} is the voltage of C at t_2 .

The angular resonant frequency of this state is: -

$$\omega_0 = \sqrt{\frac{2}{L_r C}} \quad (\text{A5})$$

The resonant impedance of this state is: -

$$Z_0 = \sqrt{\frac{2L_r}{C}} \quad (\text{A6})$$

(ii) The equations of State II [$t_1 - t_2$] are: -

$$v_C = V_{C1} \quad (\text{A7})$$

$$i_L = 0 \quad (\text{A8})$$

(iii) The equations of State III [$t_2 - t_3$] are: -

$$v_C + L_r \frac{di_L}{dt} + V_0 = 0 \quad (\text{A9})$$

$$i_L = 2C \frac{dv_C}{dt} \quad (\text{A10})$$

The solution of these two differential equations (2.9) and (2.10) are: -

$$v_C = -V_0 + (V_0 + V_{C2}) \cos \omega_1 (t - t_2) \quad (\text{A11})$$

$$i_L = -\frac{V_0 + V_{C2}}{Z_1} \sin \omega_1 (t - t_2) \quad (\text{A12})$$

where V_{C2} is the voltage of C at t_2 .

The angular resonant frequency and the resonant impedance of this state are: -

$$\omega_1 = \sqrt{\frac{1}{2L_r C}} \quad (\text{A13})$$

$$Z_1 = \sqrt{\frac{L_r}{2C}} \quad (\text{A14})$$

(iv) The equations of State IV [$t_3 - t_4$] are: -

$$v_C = V_{C3} \quad (\text{A15})$$

$$i_L = 0 \quad (\text{A16})$$

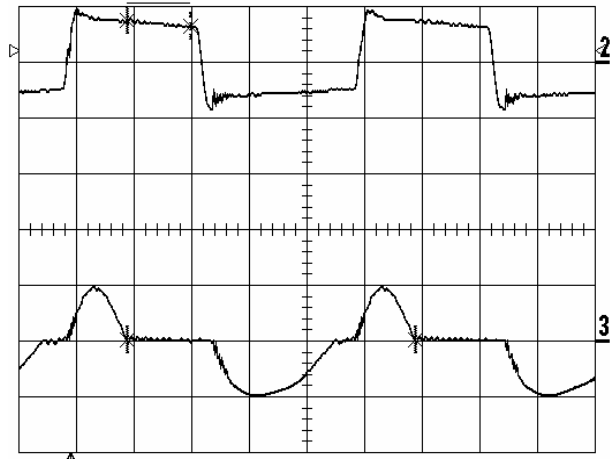
Experimental Results for 1/d mode DC-DC Switched capacitor converters

In this chapter, the both circuits of Inverting 1/2-mode step-down and resonant converter shown in Fig. A5 has been tested. The circuit is very similar to the circuit diagram that shown in Fig. A5 except that a filtering capacitor C_{in} was added to eliminate effects from the inductance of the conduction line between the power source and the input of the converter. For output voltage ripple less than 2%, specification of prototype of the circuit is shown in Table A.1.

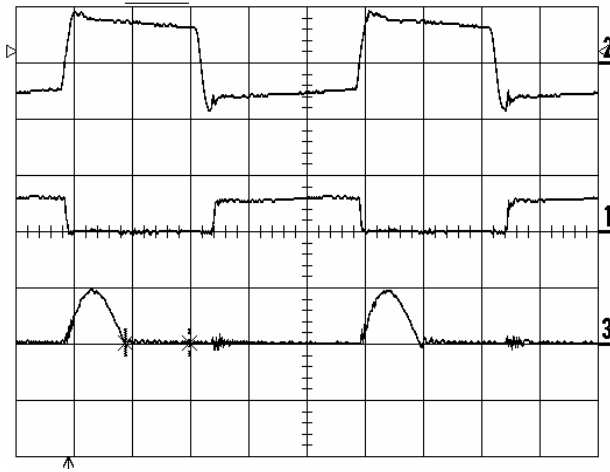
Table A.1 Specification of Prototype of Inverting 1/2-mode Converters

Descriptions	Model Numbers	Values	Units
Input Voltage	/	60	V
Expected Output Voltage	/	30	V
Switching Frequency	/	215	kHz
Output Power	/	10-60	W
S_1 and S_2	IRF630	/	/
D_{1a} , D_{1b} , D_{2a} and D_{2b}	MBR10100	/	/
C_{1a} , C_{2b}	/	0.22	μF
C_2	/	50	μF
L_r	/	1	μH

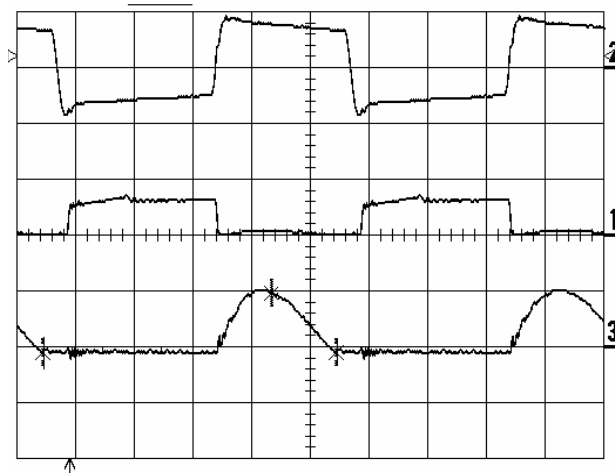
Since the main power flows through both C_{1a} and C_{2b} in the resonant state, the equivalent series resistance of these capacitors should be very low. High ESR may lead to high power loss and high temperature of the capacitors which may exceed the rated temperature of the capacitors. For this reason, polyester capacitors were chosen for these switched-capacitors.



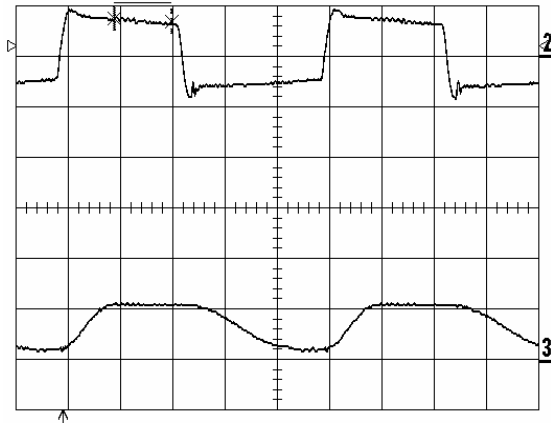
(a) Upper trace: Gate signal of S_1 , 20V/div, Lower trace: I_L , 5A/div



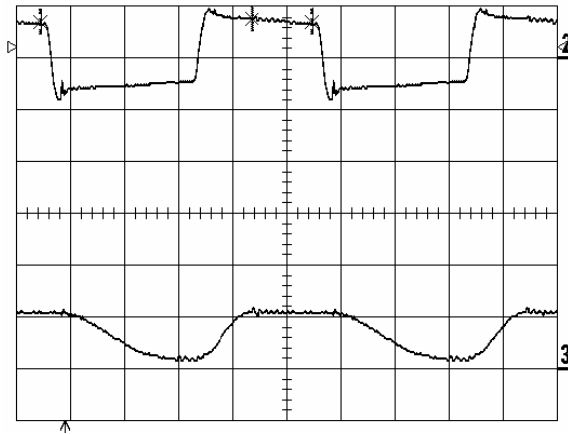
(b) Upper trace: Gate signal of S_1 , 20V/div, Middle trace: V_{ds} of S_1 , 100V/div
Lower trace: S_1 current, 5A/div



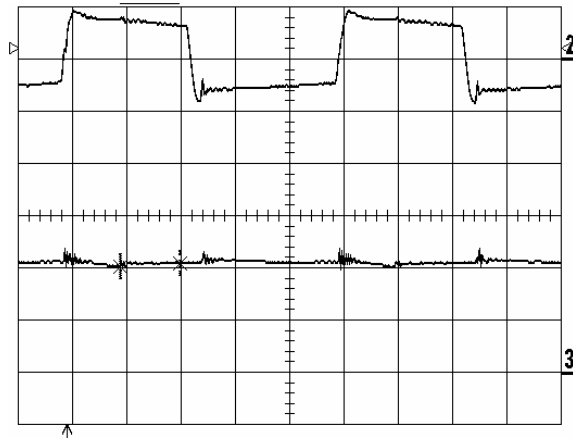
(c) Upper trace: Gate signal of S_2 , 20V/div, Middle trace: V_{ds} of S_2 , 100V/div
Lower trace: S_2 current, 5A/div



(d) Upper trace: Gate signal of S_1 , 20V/div, Lower trace: Voltage of V_{C1} , 40V/div



(e) Upper trace: Gate signal of S_2 , 20V/div, Lower trace: Voltage of V_{C2} , 40V/div



(f) Upper trace: Gate signal of S_1 , 20V/div, Lower trace : Output Voltage of V_O , 10V/div

Time base = $1\mu\text{s}/\text{div}$ for (a) to (e)

Fig. A.5 Measured waveforms of the inverting 1/2-mode switched-capacitor resonant step-down converter

Measured waveforms of the inverting 1/2-mode step-down zero-current switching quasi-resonant converter operating with 60W output power are shown in Fig. A.5. Fig. A.5(a) shows the resonant inductor current I_L . Fig. A.5(b) and Fig. A.6(c) shows the currents and drain to source voltages V_{ds} , of the transistors S_1 and S_2 . By comparing the output waveform of Fig. A.5(b) with Fig. A.5 (c), it can be observed that the resonant inductor current consists of the transistors S_1 and S_2 currents. The output voltage of the converter is shown in Fig. A.5(f). The measured output voltage of the converter was 23.45V when the output power is 60W. The measured output voltage is lower than the expected output voltage (30V) and the practical simulated output voltage because of the drain to source resistance of the transistors and the voltage drop of the diodes in forward bias. The resistance of wires and inductors, and the equivalent series resistance (ESR) of all capacitors cause an output voltage drop and power loss in the circuit. To minimise the influence of the ESR of the capacitors, polypropylene capacitors, which have low ESR, are used as the switched capacitors.

Fig. A.5(b) and Fig. A.5(c) show that the transistor currents resonate in a sinusoidal manner. The resonance stops when the current reaches zero while the drain to source voltage of the corresponding transistors is zero. The transistors are switched off when the currents are equal to zero so that zero-current switching condition is obtained. This is very similar to the simulated waveforms. Fig. A.5(d) and Fig. A.5(e) shows the voltages of switched capacitors C_{1a} and C_{2b} . The voltage waveform of C_{1a} is almost the same as that of C_{2b} . The amplitude of voltage of switched-capacitor is lower than those in simulation waveforms because of the voltage drop of the transistors, diodes and the wires.

Fig. A.6 shows the graph of the relationship between efficiency and output power of the converter. By testing the circuit with the output power between 10W to 60W, the efficiency varied around 61% to 90% at both 10W and 60W output power to 90% at 14W output power. Fig. A.7 shows the graph of voltage conversion ratio against output power of the converter. The voltage conversion ratio varies between 0.48 at 14W output power to 0.31 at 60W output power. Fig. A.6 shows that the efficiency was highest when the output power was 14W. At light load, power loss of the circuit is mainly due to the diodes, which have voltage drop in forward bias. At heavy load, the power loss is mainly due to drain-to-source resistance (R_{ds}) of the transistors. Besides, power loss occurs in the manner of switching loss of the transistors, and conduction losses of the conductor, inductor and the equivalent series resistance (ESR) of the capacitors. On the other hand, Fig. A.7 shows that the voltage conversion ratio decreases when the output power increases. Other than the voltage drop on the diodes, when the current increases, the voltage drop on both transistors increases, and, voltage conversion ratio decreases.

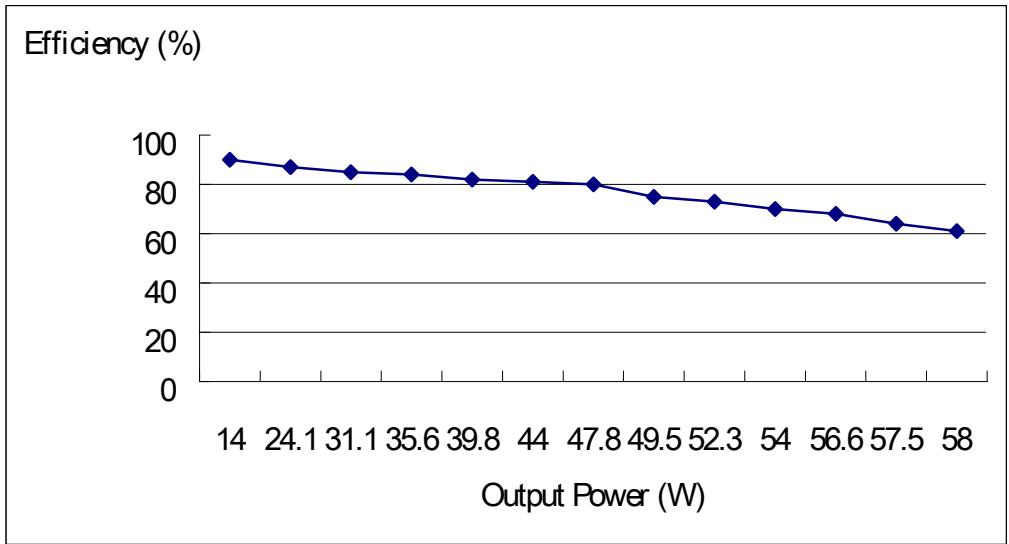


Fig. A.6 Measured efficiency and output power of the inverting 1/2-mode switched-capacitor resonant step-down converter

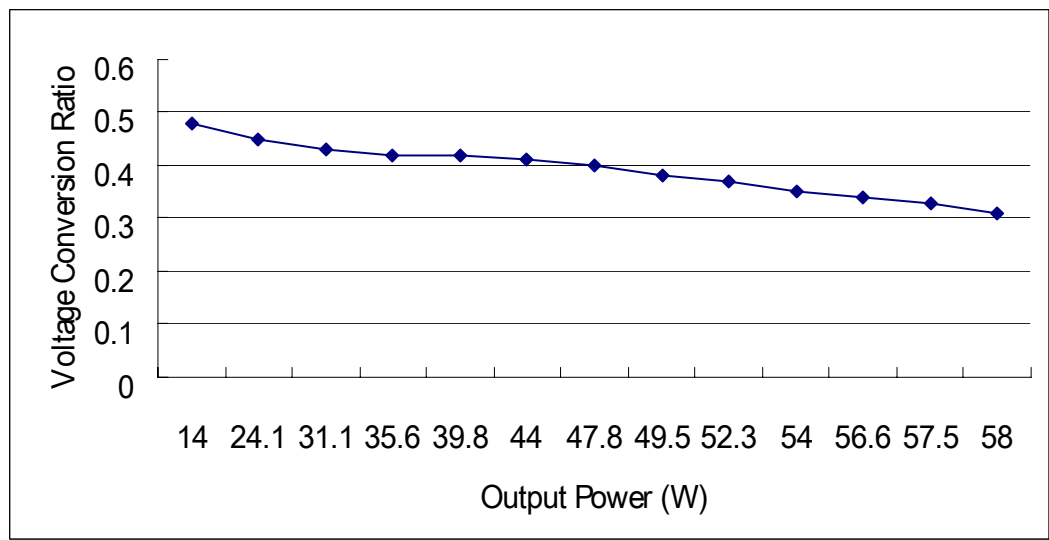


Fig. A.7 Measured voltage conversion Ratio and output power of the inverting 1/2-mode switched-capacitor resonant step-down converter

References

- 1.1 Zaohong Yang, Student Member, IEEE, and P.C. Sen, Fellow, IEEE, “Recent Developments in High Power Factor Switch-mode Converters”, IEEE. P.477-480.
- 1.2 Khalid Rustom and Issa Batarseh, “Recent Advances in Single-Stage Power Factor Correction”, IEEE, ICIT 2003 – Maribor, Slovenia. P.1089-1095.
- 1.3 R.Redl, P.Tenti and J.D. Van WYK, “Power Electronics’ Polluting Effects”, IEEE 61000-3-2 (2001-10) Consolidated Edition.
- 1.4 N. Mohan, T.M. Undeland and W.P. Robbins “Power Electronics, Converters, Applications, and Design”, John Wiley & Son, Inc., New York, 1995, 2nd Edition.
- 1.5 M.J. Kocher and RL. Steigerwald, “An AC-to-DC converter with High Quality Input Waveform”, IEEE Transactions on IA, Vol.19, No.4, P.586-599, July/August 1983.
- 1.6 Lee, F.C., Ridley, R. and Zhou, C., “Design and Analysis of a Hysteretic Boost Power Factor Correction Circuit”, IEEE P.E.S.C Proceedings, 1990.

- 1.7 C.K.Tse, S.C. Wong and M.H.L. Chow, "On Lossless Switched-capacitor Converter", 1995, 10(3), IEEE Transactions, Power Electronics, pp. 286-291.
- 1.8 Wonseok Lim , Byungcho Choi, and Yonghan Kang, "Control Design and Closed-Loop Analysis Switched-Capacitor Dc-To-Dc Converter", 2001 IEEE.
- 1.9 Cheng K.W.E., "New Generation of Switched Capacitor Converters", 1998 IEEE, PESC, pp. 1529-1535
- 1.10 K.W.E.Cheng, "Zero-Current-Switching Switched-Capacitor Converters", IEE Proc. – Electronic Power Application, Vol.148, NO. 5, September 2001.
- 1.11 Y.P.B. Yeung, and K.W.E. Cheng, " Zero-current Switching Fixed Frequency Resonant - Transition Square Wave Converters", Electronic Power Application, IEE Proc., Vol.148, No.6, P.475-480, Nov.2001.
- 1.12 Y.P.B.Yeung, K.W.E. Cheng, D. Sutanto, and S. L. Ho, "Zero-current Switching Switched-capacitor Quasi-resonant Step-down Converter", Electronic Power Application, IEE Proc., Vol.149, No 2, P.111-121, Mar 2002.

- 1.13 FRED C. LEE, senior member, IEEE, “High-Frequency Quasi-resonant Converter Technologies”, Proceedings of the IEEE, Vol.76, No. 4, April 1988.
- 1.14 Tadashi Suetsugu, “Novel PWM Control Method of Switched Capacitor DG-DC Converter”, 1998 IEEE.
- 1.15 J. Bazinct and J. O’Connor, “Analysis and Design of a Zero- voltage-Transition Power Factor Correction Circuit”, in IEEE Application Power Electronic Conference Rcc, 1994, P.591-600.
- 1.16 K.M. Smith and K.M. Smedley,”A Comparison of Voltage Mode Soft-Switching Methods for PWM Converts, “IEEE Transactions, Power Electronic, Vol.12, P.376-386, Mar1994.
- 1.17 G. Hua, C- S. Lieu, Y. Jiang, and F.C. Lee, “Novel Zero-Voltage-transition PWM Converters”, IEEE Transactions, Power Electronic, Vol.9. P.213-219, Mar.1994.
- 2.1 FRED C. LEE, senior member, IEEE, “High-frequency Quasi-resonant Converter Technologies”, Proceedings of the IEEE, vol.76, no. 4, April 1988.

- 2.2 Y.P. Benny Yeung, K.W.E. Cheng, Member, IEEE, S.L. Ho, K.K.Law and Danny Sutanto, Senior Member, IEEE, “ Unified Analysis of Switched-capacitor Resonant Converters”, 0278-0046/04 2004 IEEE.
- 2.3 K.K.Law, K.W.E.Cheng and Y.P.B.Yeung, “Design and Analysis of Switched-capacitor Based Step-up Resonant Converters”, IEEE Transactions, Circuit System I, (MNS-967).
- 3.1 K.W.E.Cheng, “Investigation of the storage energy for classical switched mode power converters”, IEE Proceedings-Electric Power Applications, Vol. 150, Issue 4, July 2003, pp. 439-446.
- 3.2 H.S.H. Chung, W.C. Chow, S. Y. R. Hui and S.T.S. Lee, “Development of A Switched-capacitor DC-DC Converter with Bi-directional Power Flow”, IEEE Transactions on Circuits and Systems1, Vol.47, No.9, P.1383-1389, Sept 2000.
- 3.3 W.S. Harris and K.D.T. Ngo, “Power Switched-capacitor DC-DC Converter: Analysis and Design” IEEE Trans., On Aerosp. And Electron System, Vol.33., No.2, P.386-395, Apr,1997.
- 3.4 C.P. Liu, Chi K. Tse, N.K. Poon, Bryan M.H. Pong and Y.M. Lai, “Synthesis of Input-Rectifierless AC/DC Converters” IEEE Transactions. On Power Electronics, Vol.19, No.1, P.176-182, Jan, 2004.

- 4.1 K.W.E.Cheng, “Zero-current-switching switched-capacitor converters”, IEE Proceedings-Electronic Power Application, Vol. 148, No. 5, Sep 2001, pp. 403-409.
- 4.2 Y.P.B.Yeung K.W.E.Cheng, S.L.Ho K.K.Law and D.Sutanto, “Unified analysis of switched-capacitor resonant converters”, IEEE Trans Ind. Electronics, Industrial Electronics, IEEE Transactions on , Volume: 51 , Issue: 4 , Aug. 2004, pp.864 – 873
- 5.1 Y.P.Yeung, K.W.E.Cheng and D.Sutanto, “Investigation of multiple output operation for switched-capacitor resonant converters”, Int.J. Cct Theory & App, Vol. 30, Issue 4, Mar 2002, pp. 411-423.